

Intracerebral Microinjection of Interleukin-4/Interleukin-13 Reduces β -Amyloid Accumulation in the Ipsilateral Side and Improves Cognitive Deficits in Young APP23 Mice

K. Kawahara,^{a,b1} M. Suenobu,^{a,b1} A. Yoshida,^a K. Koga,^a A. Hyodo,^a H. Ohtsuka,^{a,b} A. Kuniyasu,^{a,b} N. Tamamaki,^c Y. Sugimoto,^b AND H. Nakayama^{a*}

^a*Department of Molecular Cell Function, Graduate School of Medical and Pharmaceutical Sciences, Kumamoto University, 5-1 Ohe-Honmachi, Kumamoto 862-0973, Japan;*

^b*Department of Pharmaceutical Biochemistry, Graduate School of Medical and Pharmaceutical Sciences, Kumamoto University, 5-1 Ohe-Honmachi, Kumamoto 862-0973, Japan; and*

^c*Department of Morphological Neural Science, Graduate School of Medical and Pharmaceutical Sciences, Kumamoto University, 1-1-1 Honjo, Kumamoto 860-8556, Japan*

*Corresponding author: Dr. Hitoshi Nakayama, Department of Molecular Cell Function, Graduate School of Medical and Pharmaceutical Sciences, Kumamoto University, Kumamoto 862-0973, Japan. Tel: +81-96-371-4358, Fax: +81-96-372-7182. E-mail address: jin@gpo.kumamoto-u.ac.jp

¹K.K. and M.S. contributed equally to this work.

Abbreviations: A β , β -amyloid; AD, Alzheimer's disease; ANOVA, analysis of variance; APP, amyloid precursor protein; ELISA, enzyme-linked immunosorbent assay; IL, interleukin; IL-4R α , IL-4 receptor α chain; MWM, Morris water maze; NEP, neprilysin; PBS, phosphate-buffered saline; Th2, T-helper type 2; TNF- α , tumor necrosis factor- α ; TSA, tyramide signal amplification; WT, wild-type.

Abstract

We previously reported that the anti-inflammatory cytokine interleukin (IL)-4 induced selective clearance of oligomeric β -amyloid ($A\beta_{1-42}$) in rat primary type 2 microglial cells. For the present study, we investigated whether IL-4 and IL-13 could activate microglial cells to induce $A\beta$ clearance *in vivo* and improve cognitive deficits in APP23 mice, which are amyloid precursor protein transgenic mice. We administered an intracerebral microinjection of a mixture of IL-4 and IL-13 or of saline vehicle into one hemisphere of APP23 mice and their wild-type littermates, 4.5 and 9 months old, after which we evaluated the effects of these treatments on spatial learning and memory by Morris Water Maze test and on accumulated amounts of $A\beta$. The cytokine injection significantly improved memory deficits of 4.5-month-old APP23 mice, but did not do so in 9-month-old APP23 mice, even though similar $A\beta$ reductions were observed in both age groups of APP23 mice in the ipsilateral neocortex. The cytokine injection improved memory impairment of 9-month-old WT mice in the probe trial. Immunohistochemical analysis of the 4.5-month-old APP23 mice revealed the presence of increased numbers of microglial cells at 2 days after the cytokine injection. In addition to induced CD36 expression in the activated microglia, increased expression of neprilysin, mainly in neurons, suggested that the cytokines improved the cognitive deficits via degradation and clearance of intra- and extraneuronal $A\beta$ peptides, of buffer-extractable nonplaque form. Double immunostaining also revealed that most of the activated microglia had the M2-like phenotype. This unique mechanism of IL-4/IL-13-induced clearance of $A\beta$ may provide an additional strategy to prevent and/or cure Alzheimer's disease at early

stage.

Key words: Alzheimer's disease; β -amyloid; interleukin-4/interleukin-13; memory improvement; CD36; neprilysin

(Introduction)

Alzheimer's disease (AD) is an age-related progressive neurodegenerative disorder characterized by memory loss and severe cognitive decline. Morphological manifestations of clinical features include excessive accumulation of extracellular aggregations of β -amyloid ($A\beta$) peptide in the form of amyloid plaques in brain parenchyma, particularly in the cerebral cortex and hippocampus, which leads to neuronal loss (Hardy and Selkoe, 2002; Hoshi et al., 2003; Kaye et al., 2003). Promising therapeutic strategies for AD include preventing, reversing, and reducing $A\beta$ deposition.

The AD brain continues to demonstrate that innate immune responses remain active (Zelcer et al., 2007). For example, AD brains contain increased levels of inflammatory mediators, which are thought to participate in neuronal loss. Activated microglial cells and reactive astrocytes that surround senile plaques mediate local inflammatory responses (Akiyama et al., 2000). Microglial cells interact with fibrillar $A\beta$, which results in their activation and the release of various inflammatory mediators. Although microglial cells "decorate" amyloid plaques, in the AD brain these cells do not function well as phagocytes of amyloid in deposits. The reason for this finding has been suggested to be, in part, the inhibition of their phagocytic ability by a chronic inflammatory environment (Koenigsnecht-Talboo and Landreth, 2005; Hickman et al., 2008).

Multiple forms of microglial activation exist, some of which are harmful and others of

which are beneficial in AD brains (Colton et al., 2006; Town et al., 2005a). In addition, A β “immunotherapy” promotes T-helper type 2 (Th2) immune responses associated with cerebral A β clearance (Town et al., 2002; Cao et al., 2009). Interleukin (IL)-4 and other anti-inflammatory cytokines promote the alternative activation of microglial cells to Th2-responsive cells (Goerdts and Orfanos, 1999; Mantovani et al., 2002; Duffield, 2003). To better understand the mechanisms that are important to approaches to amyloid vaccines and alternatives to these approaches, a Th2-type response rather than a Th1-type response must be ensured. The current working hypothesis in AD research, especially of researchers who study amyloid vaccines, is that a shift to a Th2-type response may repair microglial dysfunction, decrease chronic inflammation, and improve A β clearance and neuroprotective mechanisms. Growing evidence indicates that alternatively activated microglial cells may serve a protective function in AD by mediating A β clearance. In fact, we recently demonstrated that IL-4 induced the clearance of oligomeric A β_{1-42} by one subtype (type 2) of primary rat microglial cells, but not type 1 microglia, via increased expression of scavenger receptor CD36 and the A β -degrading enzymes neprilysin (NEP) and insulin-degrading enzyme (Shimizu et al., 2008). However, whether the anti-inflammatory cytokine IL-4 activates type 2 microglia and induces A β clearance *in vivo* is not certain. Recent work in a model of AD showed that virus-mediated CNS expression of IL-4 results in a decrease in A β production (Kiyota et al., 2010), but the molecular mechanism of this process was not identified. With regard to the role of glial cells in particular, these researchers observed that IL-4 treatment suppressed the accumulation of microglial and astroglial cells in the

hippocampus of AD mice (Kiyota et al., 2010). However, the contribution of alternatively activated microglial cells in IL-4-induced A β clearance *in vivo* has not been clarified.

We report here that an intracerebral microinjection of a mixture of IL-4 and IL-13 into amyloid precursor protein (APP23) transgenic mice reduced the A β levels in the brain. This procedure also improved spatial learning and memory in 4.5-month-old APP23 mice. Moreover, administration of IL-4/IL-13 induced expression of CD36 in M2-like (type 2) microglial cells and NEP in neurons. Consequently, stimulation of IL-4 production in brain parenchyma or near the blood-brain barrier or blood-cerebrospinal fluid barrier may be a new therapeutic approach for AD.

1. EXPERIMENTAL PROCEDURES

1.1 Animals

Hemizygous APP23 mice, which overexpress human-type APP and carry a double mutation (K670N/M671L), were generated and bred as previously described (Sturchler-Pierrat et al., 1997). Mice were housed in standard cages under conventional laboratory conditions (food and water available *ad libitum*, constant room temperature and humidity, 12/12-h light-dark cycle). The animal experiments were conducted according to the guidelines of the Kumamoto University Animal Committee.

1.2 Intracerebral microinjection of a mixture of IL-4 and IL-13

APP23 mice start to form amyloid deposits at 6 months of age, but their memory deficits in the Morris water maze (MWM) test manifest quite early (<3 months) (Dam et al., 2003). In this study, we used two age groups (4.5 and 9 months old) of male APP23 mice and their wild-type (WT) littermates (C57BL/6J). Four to six mice per cage were divided into two groups by stratified random sampling to equalize the mean body weight of the two study groups: mice given the IL-4/IL-13 microinjection and mice given the saline injection. Mice were anesthetized with Avertin [1.25% (w/v) 2,2,2-tribromoethanol plus 2.5% (v/v) 2-methyl-2-butanol, given at 0.375 ml/25 g body weight] and were placed in a stereotaxic apparatus with a mouse adaptor (Narishige Co. Ltd., Tokyo, Japan). We injected the left cerebral cortex of each mouse with 0.5 μ l of the mixture of recombinant murine IL-4 and murine IL-13 (each at 0.1 mg/ml: 50 ng of

IL-4 and 50 ng of IL-13 in 0.5 μ l; PeproTech EC, London, UK) or saline, which we administered by applying pressure through a glass capillary pipette. The coordinates from bregma were -0.6 mm posterior, -1.6 mm lateral, and -0.8 mm ventral to the skull (Paxinos and Franklin, 2004). Injections were given over 10 min, and the pipettes were left in place for an additional 5 min to allow for diffusion. Mice were kept on a warming pad until they recovered from anesthesia and then were monitored daily until they were killed for tissue processing. We injected IL-4/IL-13 into the cerebral cortex, because accumulation of A β plaques is reported to start earlier in cerebral cortex than in hippocampus (Roder et al., 2003; Capetillo-Zarate et al., 2006). In addition, loss of basal forebrain cholinergic neurons reportedly plays a prominent role in cognitive deficits in AD patients (Cullen and Halliday, 1998), and the importance of neocortical cholinergic neurons in MWM performance is well established (Winkler et al., 1995). We left the right brain untreated (no injection) as an internal standard for A β quantification. We confirmed that an intracerebral injection of India ink (0.5 μ l) into one hemisphere of two mice (with the injection site at -0.6 mm posterior, -1.6 mm lateral, and -0.8 mm ventral from the bregma) did not diffuse to the other hemisphere, although it did diffuse not only to the cerebral cortex but also to the lateral ventricle and corpus callosum of the ipsilateral side (data not shown).

1.3 The MWM test

Spatial learning and memory were evaluated by means of the MWM test (Morris, 1984). The test, performed during the dark cycle, utilized a circular, 150-cm-diameter

pool (height: 40 cm) that was filled with water kept at 23.0 ± 1 °C. A round platform (12 cm in diameter) was placed in one of the quadrants and was submerged 1 cm below the water surface. Acquisition training consisted of three to five trials per day for 4 consecutive days (day 1: 3 trials, day 2: 3 trials, day 3: 5 trials, and day 4: 4 trials). The trials were started from three different positions in semirandom order with a 20-min intertrial interval. A mouse that failed to find the platform within 120 s was guided carefully to the platform and allowed to stay on it for 20 s. The acquisition phase was followed by a probe trial: the platform was removed from the maze, and animals were allowed to swim freely for 100 s. During both acquisition and probe trials, the trajectories of the animals were recorded by using a computerized video tracking system (CompACT VAS; Muromachi Kikai Co. Ltd., Tokyo, Japan). During training trials, the latency to find the escape platform was measured. Probe trials measured the percentage of time spent in each quadrant of the MWM. The number of crossing over the training annulus (22 cm in diameter), which was $3.1 \times$ the size of the target platform, was also used for analysis of performance in the probe trial. In this study, probe trial was administered at 2 hours after the last training trial; therefore, it is considered that retention of spatial memory for the platform position reflects a short-term memory (Vorhees and Williams, 2006). During the MWM test, some APP23 mice showed low locomotive activity (swimming speed below the 0.06-m/s threshold). These mice were excluded from the analysis of the cytokine and saline groups (behavior).

1.4 Immunohistochemical analysis

After the behavioral study for 4 days (i.e., at 7 days after the microinjection), or 2 days after the microinjection, for A β immunostaining or other immunostainings, respectively, mice were anesthetized with pentobarbital, and 4% paraformaldehyde in phosphate-buffered saline (PBS) was perfused through the left cardiac ventricle. Brains were removed and cryoprotected in sucrose. Frozen sections (10 μ m thick, or 20 μ m thick for A β staining) were cut with a cryostat and thaw-mounted on gelatin-coated slides. The coronal sections were immersed in 10 mM citrate buffer (pH 6.0) and were autoclaved (at 80 °C) for 5 min. For CD163 and Ym1 staining, sections were autoclaved at 120 °C for 5 min. For A β staining, sections were immersed in 70% formic acid [for biotin-conjugated mouse anti-A β ₁₇₋₂₄ monoclonal antibody (b4G8)] or 70% formic acid/trypsin (for BA27 and BC05) for 10 min. Slides were then cooled for 20 min at room temperature before they were washed in PBS. Fixed sections were incubated at room temperature for 1 h in buffer A (PBS containing 0.3% Triton X-100, 1% normal donkey serum, 0.02% NaN₃, and 0.25% λ -carrageenan), followed by an overnight incubation in one of the following antibodies: b4G8, 1:500 dilution; Covance, Berkeley, CA), mouse anti-A β _{x-40} monoclonal antibody (BA27, Wako Pure Chemical Industries, Osaka, Japan), mouse anti-A β _{x-42} monoclonal antibody (BC05, Wako Pure Chemical Industries), mouse anti-synaptophysin monoclonal antibody (SY38, 1:50 dilution; Progen Biotechnik, Heidelberg, Germany), mouse anti-neuronal nuclei (NeuN) monoclonal antibody (MAB377, 1:200 dilution; Millipore, Billerica, MA), rat anti-CD68 monoclonal antibody (FA-11, 1:100 dilution; Serotec Ltd., Oxford, UK), rabbit anti-IL-4 receptor α chain (IL-4R α) antibody (S-20, 1:200 dilution; Santa Cruz

Biotechnology, Santa Cruz, CA), rabbit anti-CD163 antibody (M-96, 1:50 dilution; Santa Cruz Biotechnology), rabbit anti-arginase I antibody (1:300 dilution; a generous gift from Prof. M. Gotoh, Kumamoto University, Kumamoto, Japan) (Sonoki et al., 1997), goat anti-Ym1 antibody (AF2446, 4 μ g/ml; R&D Systems, Inc., Minneapolis, MN), or rabbit anti-Iba1 polyclonal antibody (1:500 dilution; Wako Pure Chemical Industries). After excess antibody was washed out with PBS, sections were incubated for 2 h with the corresponding Alexa Fluor 488- or 594-labeled secondary antibodies (1:400 dilution; Molecular Probes, Eugene, OR). Thioflavin S staining to visualize amyloid fibrils was performed according to the manufacturer's instructions (Sigma-Aldrich Inc., St. Louis, MO). Specimens were mounted with Dako fluorescent mounting medium (DakoCytomation, Kyoto, Japan) and were examined with a confocal laser-scanning microscope (FluoView; Olympus, Tokyo, Japan).

To visualize the label in some sections, the avidin-biotin peroxidase technique was used. After excess antibody was washed out with PBS, sections were incubated for 1 h with the corresponding biotinylated secondary antibody (1:200 dilution; Chemicon International, Inc., Temecula, CA). The sections were then incubated for 30 min at room temperature with avidin-peroxidase complex (Vector Laboratories, Inc., Burlingame, CA). The presence of peroxidase was revealed by incubation with a diaminobenzidine solution with nickel enhancement.

For immunohistochemical staining with CD36 and NEP, we used a highly sensitive tyramide signal amplification (TSA) system (Molecular Probes) according to the manufacturer's recommendations. Endogenous peroxidase was blocked by treatment

with 1% H₂O₂ in methanol for 15 min. Sections were preincubated in buffer A for 30 min, followed by overnight incubation at 4 °C with rat anti-mouse CD36 monoclonal antibody (MAB2519, 1:100 dilution; R&D Systems) or mouse anti-CD10/NEP monoclonal antibody (56C6, 1:200 dilution; Novocastra Laboratories, Newcastle upon Tyne, UK). Sections were then incubated for 30 min at room temperature with horseradish peroxidase-linked goat anti-rat or anti-mouse IgG (Nichirei, Tokyo, Japan). Sections were developed with the TSA Fluorescein System (Molecular Probes) or the diaminobenzidine-nickel substrate using TSA and the avidin-biotin-peroxidase method (Vector Laboratories).

A β quantification was performed as described previously (Oddo et al., 2004). Brains were excluded from the immunohistological analysis if they had high nonspecific background staining for b4G8 or BA27. Microphotographs were taken, with an Olympus digital camera, of the neocortical area (layer V) surrounding the site of injection and similar areas 10 sections away from that site (with each section being 20 μ m thick). The same process was used for the contralateral side. After the photomicrographs were imported into the National Institutes of Health (NIH) Scion Image system, they were quantified via the NIH Image-J software obtained from a public website (<http://rsb.info.nih.gov/nih-image/>). A manually set threshold intensity was kept constant, and the number of pixels in A β -immunostained sections in an area measuring 550 \times 1100 μ m² (surrounding the injection site) was determined.

1.5 Enzyme-linked immunosorbent assay (ELISA)

Seven days after intracerebral injection of IL-4/IL-13 or saline, the ipsilateral neocortex and the contralateral area were dissected. For A β quantification, the cerebral cortex was homogenized in 10 volumes (w/v) of guanidine buffer (6.0 M guanidine hydrochloride/50 mM Tris-HCl, pH 8.0, containing 1 mM phenylmethylsulfonyl fluoride, 1 μ g/ml leupeptin, 1 μ g/ml pepstatin A, and 10 μ g/ml soybean trypsin inhibitor). The sample was centrifuged at 200,000 g for 20 min at 4 °C; the supernatant was then diluted 12 times to reduce the guanidine hydrochloride concentration. The amounts of A β ₄₂ and A β ₄₀ were determined by means of sandwich ELISAs (290-62601 and 294-64701, respectively; Wako Pure Chemical Industries), according to the manufacturer's instructions.

To quantify the endogenous A β in WT mice, the cerebral cortex was homogenized in 5 volumes (w/v) of TBS buffer (50 mM Tris-HCl, pH 8.0, containing 150 mM NaCl, 1 mM phenylmethylsulfonyl fluoride, 1 μ g/ml leupeptin, 1 μ g/ml pepstatin A, and 10 μ g/ml soybean trypsin inhibitor). The sample was centrifuged at 20,000 g for 20 min at 4 °C; the supernatant was then removed. The amounts of A β ₄₂ were determined according to the manufacturer's instructions, by means of a sandwich ELISA (292-64501; Wako Pure Chemical Industries), which shows higher sensitivity than the ELISA kit 290-62601 (see above) used for APP23 mice.

To quantify tumor necrosis factor- α (TNF- α), the cerebral cortex was homogenized in 10 volumes (w/v) of PBS buffer (PBS containing 1 mM phenylmethylsulfonyl fluoride, 1 μ g/ml leupeptin, 1 μ g/ml pepstatin A, and 10 μ g/ml soybean trypsin inhibitor). The sample was centrifuged at 10,000 g for 10 min at 4 °C; the supernatant was then

removed. The amounts of TNF- α were determined by means of a sandwich ELISA (KMC3011; BioSource International, Inc., Camarillo, CA), according to the manufacturer's instructions. Protein concentrations were determined with the Bradford protein assay reagent (Thermo Fisher Scientific Inc., Rockford, IL), with bovine serum albumin as the standard.

1.6 Statistical analysis

All data were expressed as means \pm SEM. For statistical comparisons of the means between two groups, Student's *t*-test was applied after equality between the variances of the groups was confirmed. In a factorial model analysis of variance (ANOVA), the cytokine treatment (IL-4/IL-13 vs. saline) was used as a between-subject factor and the training regimen (days or trials) was used as a within-subject (repeated measure) factor. For comparisons of three or more groups, Dunnett's multiple comparison test was used after one-way ANOVA. To determine whether a correlation existed between variables, data were analyzed via scatterplot and Pearson correlation analyses. All statistical analyses were performed with GraphPad Prism (GraphPad Software, Inc., La Jolla, CA). Significance was defined as *P* values of less than 0.05.

2. RESULTS

2.1 Intracerebral microinjection of IL-4/IL-13 reversed spatial learning and memory deficits in 4.5-month-old APP23 mice

APP23 mice reportedly showed an increase in A β deposition with age and displayed age-related deficits in learning and memory even at 3 months old (Dam et al., 2003). In our present study using APP23 mice of 4.5- and 9-month-old, we also observed that the age-related impairment of learning and memory and A β accumulation: A β was accumulated but no amyloid plaque was present at 4.5 months old, while deposition of amyloid plaque was abundant at 9 months-old (data not shown). We first investigated effect of IL-4/IL-13 microinjection on spatial learning and memory ability by the MWM test. We used a mixture of IL-4 and IL-13, because IL-13 shares a receptor with IL-4 and was expected to act similarly and/or additionally to IL-4, as shown in previous *in vitro* studies (Shimizu et al., 2008).

At the age of 4.5 months, saline-injected APP23 mice had already exhibited considerable impairment of acquisition of spatial learning (had a longer escape latency) in the MWM test, compared with WT littermates (Fig. 1A, and $P < 0.001$ by two-way ANOVA). In contrast, injection of IL-4/IL-13 led to a significant improvement in this measurement, compared with saline-injected control APP23 mice (two-way ANOVA: $P < 0.001$, Fig. 1A).

After the acquisition trials, mice were subjected to probe trials (Fig. 1B). On the

percentage of time spent searching in the quadrant where the hidden platform had been located, saline-injected APP23 mice showed a low score of time spent in the target quadrant ($17 \pm 3.5\%$) (Fig. 1Ba), as expected, compared with that of saline-injected WT mice ($39 \pm 6.1\%$) (Fig. 1Bb, and $P < 0.05$ by post hoc Dunnett's multiple comparison test). After the IL-4/IL-13 injection, however, APP23 mice spent significantly longer time in the target quadrant ($29 \pm 3.0\%$) than did the saline-injected APP23 mice (Fig. 1Ba). For the number of crossings over the training annulus, a similar improvement was observed in IL-4/IL-13-injected APP23 mice (Fig. 1Ca). In contrast, microinjection of IL-4/IL-13 had little effect on 4.5-month-old WT littermates, as expected (Fig. 1Bb, 1Cb). These results indicate that memory deficits of 4.5-month-old APP23 mice were apparently reversed by intracerebral microinjection of IL-4/IL-13.

At the age of 9 months, APP23 mice (saline-injected) showed more impairment of acquisition of spatial learning than the 4.5-month-old mice, compared with the corresponding WT littermates (Fig. 2A, $P < 0.001$ by two-way ANOVA). Even after the cytokine-injection, the 9-month-old APP23 mice showed no improvement in the behavioral tests: $P = 0.324$ for the acquisition trials (Fig. 2A) by two-way ANOVA, and $P = 0.452$ and $P = 0.284$ for the probe trial (Fig. 2Ba, 2Ca). We mention that these data include larger statistic deviations than those of 4.5 month-old APP23 mice, and they hamper the positive judgment that the cytokine treatment is also effective to memory improvement in 9 month-old APP23 mice.

In the non-transgenic 9-month-old WT littermates, however, microinjection of IL-4/IL-13 resulted in a significantly improved spatial memory in the probe trial,

compared with the saline-treated control ($P < 0.001$, in Fig. 2Bb, 2Cb), but this effect was not apparent in the escape latency of training trial (Fig. 2A). This result suggests that memory formation process of 9-month-old WT mice (measured by training trials) is normal, but their retention of spatial memory for the platform position (measured by probe trial) is impaired, until the IL-4/IL-13-injection improves it.

2.2 Memory improvement of IL-4/IL-13-injected 4.5-month-old APP23 mice was correlated with reduced A β peptide levels in brain

In view of the memory improvement obtained by IL-4/IL-13 microinjection, sections of the brain from 4.5-month-old APP23 mice were studied to determine whether the cytokine microinjection could reduce the amount of A β in the brain. Coronal slices of brain from cytokine-injected and saline-injected mice were immunostained with the b4G8, which reacts with almost all A β forms including A β_{1-42} , A β_{1-40} , and full-length APP (data sheet no. SIG-39240, Covance). The intensity of immunostaining in the neocortical area surrounding the injection site (ipsilateral side) was compared with that in the contralateral side. We found a decrease of the b4G8⁺ A β level in the ipsilateral neocortex of IL-4/IL-13-injected mice compared with the contralateral side (Fig. 3A). Quantitative analysis also showed significantly reduced b4G8 immunoreactivity in the ipsilateral neocortex of the cytokine-injected group compared with the saline-injected group ($P = 0.001$, Fig. 3Ba). In addition, a post hoc comparison indicated that a significant decrease was observed only in the ipsilateral side of the cytokine-injected

group ($P < 0.05$, Fig. 3Ca). The 9-month-old IL-4/IL-13-injected APP23 mice also had a significant reduction in b4G8 immunoreactivity in the neocortex compared with the saline-injected group ($P = 0.012$, Fig. 3Bb). A post hoc comparison, however, showed a statistically insignificant change because of a large variation in values (Fig. 3Cb).

To further investigate the effect of IL-4/IL-13 microinjection on different species of A β peptides, we subjected the continuous coronal sections that were shown in Fig. 3 to immunostaining with the antibodies BA27 and BC05, which specifically recognize A β_{40} and A β_{42} (Iwatsubo et al., 1994), respectively. The BA27⁺ A β_{40} level in the neocortex of 4.5-month-old APP23 mice, like the total A β level immunostained with 4G8, was significantly reduced by the IL-4/IL-13 injection, compared with that in the saline-injected group (Fig. 4A, 4B). In 9-month-old APP23 mice, the IL-4/IL-13 injection significantly reduced BA27 immunoreactivity in the ipsilateral neocortex compared with the saline injection (Fig. 4C, 4D).

With regard to A β_{42} immunostaining in 4.5-month-old APP23 mice, the level was below the detection limit for BC05 immunostaining (data not shown). Therefore, we quantified the amounts of A β_{42} and A β_{40} by means of sandwich ELISA for both ipsilateral and contralateral sides of the neocortex of 4.5-month-old APP23 mice and compared the results for the IL-4/IL-13-injected and saline-injected groups. Figures 5A and 5B show that the cytokine injection significantly reduced the amounts of both A β_{42} and A β_{40} peptides to a similar extent ($74 \pm 4.3\%$ and $76 \pm 7.0\%$, respectively) and only in the ipsilateral neocortex. In addition, relationship between the A β_{42} level in the ipsilateral side of IL-4/IL-13-injected mice and performance in the MWM showed a

significant correlation ($P=0.007$) with a negative slope ($r= - 0.817$), while no apparent correlation was observed in the saline-injected groups ($P=0.817$, $r=-0.090$), as shown in Fig. 5C. The ELISA method also demonstrated that the amount of endogenous $A\beta_{42}$ that accumulated at low level (~ 2 fmol/mg) in the neocortex of 9-month-old WT mice was reduced significantly ($P=0.038$) by the IL-4/IL-13 injection, compared with the saline injection (Fig. 5D).

2.3 IL-4/IL-13 microinjection activated microglial cells and induced CD36 and NEP in 4.5-month-old APP23 mice

We previously reported that CD36 and NEP contributed to IL-4-induced degradation of oligomeric $A\beta_{1-42}$ in rat type 2 microglial cells *in vitro* (Shimizu et al., 2008). To determine whether microglia and these molecules are also involved in the observed reduction in $A\beta$ *in vivo*, we inspected the change in the microglial/macrophage marker Iba1, and then the expression and distribution of CD36 and NEP, by means of immunohistochemical staining of brain slices at various time points after IL-4/IL-13 microinjection. Iba1 staining (Fig. 6) showed that the cytokine microinjection caused microglial cells in the ipsilateral side to change morphology, to an activated phenotype with thick processes, although cell numbers showed no change at day 1. Two days after the injection, number of the activated microglial cells increased in the ipsilateral side. The change in morphology and the increased number of microglial cells returned to basal levels at 4 days after the injection. The saline-injected group did not show these

changes in Iba1⁺ cells (Fig. 6B). In addition, the increased number of microglial cells at 2 days after the cytokine injection was statistically significant compared with the number of microglial cells in the saline-injected group ($P < 0.001$), as Fig. 6C shows.

Immunoreactivity of CD36 and NEP also increased at 2 days after the IL-4/IL-13 injection (Fig. 7A, 7B). To determine whether microglial cells actually expressed CD36 and NEP, we used double immunostaining of brain slices at 2 days after the cytokine injection. As seen in Fig. 8A, CD36⁺ cells colocalized with several Iba1⁺ microglial cells. NEP⁺ cells were also observed in the cortical slices, and some NEP⁺ cells colocalized with Iba1⁺ cells (Fig. 8B). Therefore, some Iba1⁺ microglial cells expressed NEP. However, the population of NEP⁺ cells was apparently larger than the Iba1⁺ cell population, which suggests that cells other than microglial cells express the majority of NEP. Because most NEP⁺ cells colocalized with the neuronal presynaptic marker synaptophysin in the cortical slices (Fig. 9A), the majority of NEP⁺ cells were identified as neurons. In addition, we found that IL-4R α , a co-receptor for IL-4 and IL-13, was mainly induced in the CD68⁺ microglial cells of the ipsilateral side at 2 days after IL-4/IL-13 injection (Fig. 9B).

Together, these results strongly suggest that microinjection of IL-4/IL-13 activates IL-4R⁺ microglial cells to induce expression of both CD36 and NEP. IL-4 and IL-13 are also thought to affect neurons indirectly and enhance NEP expression (this point is discussed in more detail later).

2.4 IL-4/IL-13 microinjection induced alternative microglial activation

In this study, we also identified that the anti-inflammatory phenotype of microglial cells was activated by IL-4/IL-13 microinjection. Arginase I, CD163, and Ym1, all of which are markers for the anti-inflammatory, alternatively activated phenotype (M2-like microglia), were induced in the ipsilateral neocortex at 2 days after the cytokine microinjection (Fig. 10A-10C), but they were undetectable after injection of vehicle. We confirmed that the M2-related protein Ym1 was induced in Iba1⁺ microglial cells of the ipsilateral side at 2 days after the cytokine injection (data not shown). In addition, cytokine-induced CD36 expression was observed in the arginase I-positive and Ym1⁺ cells, which indicates that CD36⁺ microglial cells are M2-like cells (Fig. 10D, 10E). Furthermore, the IL-4/IL-13 injection reduced the TNF- α level in the ipsilateral neocortex of 4.5-month-old APP23 mice, compared with saline-injected mice (Fig. 11A). The TNF- α levels in the ipsilateral side and the performance in MWM (the percentage of time spent in target quadrant) showed a significant relationship ($P=0.031$) with a negative correlation ($r=-0.969$) in the IL-4/IL-13-injected mice (Fig. 11B), while no such correlation was observed in the saline-injected groups ($P=0.428$, $r=0.572$, Fig. 11B). These results indicate that IL-4/IL-13 suppressed TNF- α production and promoted anti-inflammatory action in microglial cells in 4.5-month-old APP23 mice.

3. DISCUSSION

Previous *in vitro* observations, in which treatment with the anti-inflammatory cytokine IL-4 induced selective clearance of oligomeric A β ₄₂ in type 2 microglial cells (Shimizu et al., 2008), led us to undertake this study, in which we examined whether A β clearance actually reduced learning and memory deficits *in vivo* in APP23 mice, which are APP transgenic mice. A single microinjection of IL-4/IL-13 did indeed reduce the total A β levels in the cerebral cortex (Fig. 3B) of APP23 mice of both tested ages (4.5 and 9 months). However, a significant improvement in memory deficits was observed only in 4.5-month-old mice, not in 9-month-old mice.

3.1 Different effects of IL-4/IL-13 on memory improvement in APP23 mice of different ages and possible relations to A β forms reduced

A β deposition in the brain of APP23 mice reportedly increases with age, and mice manifest age-related learning and memory deficits (Dam et al., 2003). In our study using APP23 mice here, we observed that considerable amount of the total A β (b4G8⁺) accumulated in the 4.5-month-old mice and it increased even more in the 9-month-old mice (1.5-fold relative to the 4.5-month-old mice) (Fig. 3B). Learning and memory were already consistently impaired in the 4.5-month-old mice (Fig. 1A), and the 9-month-old mice showed somewhat greater impairment (Fig. 2A). A notable observation is that A β plaques, which were not seen in 4.5-month-old mice, but were obvious in 9-month-old mice (Fig. 4C, 4D). However, microinjection of IL-4/IL-13

apparently reduced total A β levels in the ipsilateral neocortex to a similar extent in both ages of APP23 mice (Figs. 3 and 4), although the cytokine treatment improved spatial memory only in the 4.5-month-old mice. Consequently, we inspected the A β forms reduced, and found that they were nonplaque A β , but not A β plaques, as shown in Fig. 4A and 4C.

Therefore, the behavioral improvements by cytokine injection may reflect the efficient removal of soluble or intra- and extraneuronal A β s, which are thought to contribute to pathological dysfunction of learning and memory in 4.5-month-old mice, whereas in 9-month-old mice, the accumulated insoluble plaques may play a dominant pathological role in chronic memory deficits. With regard to the A β form that was reduced in 9-month-old APP23 mice by the cytokine microinjection, the belief is that this A β did not consist of insoluble plaques but rather was a smaller species (Fig. 4C, 4D), possibly soluble A β , because similar degrees of A β reduction were observed in the cytokine-treated 4.5-month-old APP23 mice (an age before A β plaque formation occurs) by means of the immunostaining (Fig. 4A, 4B) and the ELISA of buffer-extracted A β fractions (Fig. 5). It is of notice that the reduction of buffer-extractable A β_{42} is well correlated with the memory improvement in 4.5 month-old APP23 mice (Fig. 5C). Consequently, this microinjection was more effective for 4.5-month-old APP23 mice, in which nonplaque, soluble A β species are dominant, than for 9-month-old APP23 mice, in which insoluble A β plaques are abundant. We previously demonstrated that IL-4-induced A β clearance by type 2 microglial cells was selective for the oligomeric A β form (Shimizu et al., 2008), and we attempted to

determine the content of oligomeric A β in brain slices from APP mice of both ages by using an oligomer-specific antibody (Kayed et al., 2003). However, this attempt was unsuccessful, possibly because the A β oligomers in the samples were present at a level lower than the detection limit of the antibody. Therefore, further study is needed to verify whether oligomeric A β is responsible for the memory deficiency and its improvement via cytokine treatment *in vivo*.

With regard to the location of A β , which was accumulated in 4.5-month-old APP23 mice and reduced by the cytokine injection, we observed that a considerable amount of A β was located in neurons (data not shown). That no extraneuronal A β was observed in 4.5-month-old APP23 mice may reflect the results that glial cells such as microglia are highly efficient in degrading it (Matsunaga et al., 2003) and that neurons internalize A β from the extracellular milieu (Mohamed and Posse de Chaves, 2011). In 9-month-old APP23 mice, A β was mainly accumulated in the extracellular space as A β plaques, and insoluble A β plaques rather than soluble A β are thought to be critically involved in chronic memory deficits. Continuous administration of IL-4/IL-13 by means of the virus-mediated transduction reported by Kiyota et al. (Kiyota et al., 2010), rather than the single injection that we employed, may reduce A β plaque levels enough to improve memory impairment even in 9-month-old APP23 mice. Additional studies of this issue are required.

In our study here, the IL-4/IL-13 microinjection also significantly enhanced spatial memory retention in 9-month-old WT mice in a probe trial but produced no significant improvement in escape latency (Fig. 2A, 2B). This improvement was not observed in

the younger, 4.5-month-old WT mice (Fig. 1B). We also observed that the amount of endogenous $A\beta_{42}$ that accumulated in the neocortex of 9-month-old WT mice was reduced by the IL-4/IL-13 injection (Fig. 5D), although the amount of accumulated $A\beta_{42}$ (~2 fmol/mg) was much lower than that of 4.5-month-old APP23 mice (~ 0.1 pmol/mg). All these results suggest that 9-month-old WT mice may be at an early neuropathological stage, but they may not show the AD pathology as observed in the APP23 mice, because the accumulation level of $A\beta$ was very low.

At the early pathological stage of 9 month-old WT mice, we consider that age-related inflammatory changes in hippocampus may be participated. Reportedly, the brain inflammation causes deficits in synaptic function to lead impairments of cognitive function. For example, peripheral administration of lipopolysaccharide (LPS) increased pro-inflammatory cytokine interleukin-1 β (IL-1 β) concentration in the brain, and led to the impairment of hippocampal-dependent learning and memory (Shaw et al., 2001). Nolan et al (2005) further showed that intracerebroventricular injection of IL-4 restored synaptic functions in aged rats and in LPS-treated rats, in both of which IL-1 β concentrations had been enhanced. Derecki et al (2010) recently reported that IL-4 knock-out mice showed higher levels of TNF- α in hippocampus and cognitive impairment in MWM test when compared with their WT controls, but these changes were reversed by adaptive transfer of T cells from WT mice. Therefore, the mechanism that the inflammation-related memory impairment was reversed by IL-4, may participate in the present memory improvement of 9-month-old WT mice after IL-4/IL-13 injection. It will be necessary, however, to examine them in future.

3.2 Proposed mechanisms of A β clearance

Our work described herein partly elucidates the possible mechanisms by which IL-4/IL-13 reduced the A β level *in vivo*, inasmuch as microglial activation including enhanced expression of CD36, and elevated NEP primarily in neurons were detected only in the ipsilateral side of the neocortex given the IL-4/IL-13 microinjection.

We previously showed that CD36 and NEP contributed to IL-4-induced degradation of A β in rat primary type 2 microglial cells *in vitro* (Shimizu et al., 2008). In the present study, we also detected transient activation of these cells at 2 days after an IL-4/IL-13 microinjection, with enhanced expression of CD36 and NEP in the ipsilateral side of the neocortex. Double-immunostaining experiments revealed obvious induction of CD36 in the activated microglial cells (Fig. 8A), whereas greater NEP expression was observed in synaptophysin-positive neurons than in activated microglial cells (Fig. 8B and Fig. 9A). The extra- and intracellular pools of A β are related and affect each other via intracellular and extracellular equilibria of A β peptides (Yang et al., 1999; Oddo et al., 2006; Tampellini et al., 2009). A decrease in extracellular A β via microglial clearance reportedly led to a reduction in the intracellular A β pool (Schenk et al., 1999; Butovsky et al., 2007; El Khoury et al., 2007). Therefore, our results suggest that CD36, which is enhanced in activated microglial cells, effects A β clearance, which leads to intraneuronal A β reduction via possible wide-range equilibria between extra- and intraneuronal A β peptides, whereas NEP, which is enhanced mainly in neurons and partly in microglial cells, contributes to degradation of accumulated A β .

IL-4 receptors were reportedly expressed in granule cells of the dentate gyrus (Nolan et al., 2005), but IL-4 had no effect on NEP expression in primary cortical neurons (Saito et al., 2005). In our study here, we determined that IL-4R α , which is a co-receptor for IL-4 and IL-13, was mostly induced in CD68⁺ microglia/macrophages in the ipsilateral neocortex at 2 days after IL-4/IL-13 injection (Fig. 9B). This result suggests that microglial CD36 and NEP are induced in IL-4R α ⁺ microglial cells via an IL-4R-mediated process. For the NEP that is enhanced in neurons, however, we believe that its expression may be stimulated by a microglia-neuron interaction, because most of the IL-4R α was expressed in activated microglia and no obvious IL-4R α expression was observed in neurons (Fig. 9). The possibility of such a microglia-neuron interaction warrants further study, however.

3.3 Anti-inflammatory roles of IL-4/IL-13 in the CNS

Local microenvironments favor an association of A β with macromolecules, such as apolipoproteins and extracellular matrix components, which leads to formation of compact plaques (Bales et al., 1999; Kim et al., 2009). Inflammatory conditions in brain also lead to the formation of densely compacted senile plaques (McGeer and McGeer, 2001). Conversely, anti-inflammatory IL-4 and IL-13 induce A β clearance in microglial cells (Shimizu et al., 2008; Yamamoto et al., 2008), whereas pro-inflammatory cytokines reduce such clearance (Koenigsknecht-Talboo and Landreth 2005; Hickman et al., 2008). IL-4 suppressed *in vitro* microglial production of interferon- γ -induced TNF- α (Colton et al., 2006), MHC class II molecules (Suzumura et al., 1994), nitric

oxide (Chao et al., 1993), and IL-6 (Szczepanik et al., 2001). In this study, we demonstrated that IL-4/IL-13 reduced A β levels in APP23 mice. In addition, we showed that CD36 and IL-4R α , which are markers for the alternatively activated microglial cells (M2-like microglia) having anti-inflammatory action, were induced in Iba1⁺CD68⁺ microglial cells by IL-4/IL-13 microinjection (Fig. 8 and Fig. 9B). Arginase I, Ym1, and CD163, which are additional markers for M2-like microglia, were also induced by the IL-4/IL-13 microinjection (Fig. 10). Furthermore, we demonstrated that IL-4/IL-13 microinjection significantly reduced the level of TNF- α , a marker for the pro-inflammatory phenotype of microglial cells (M1-like microglia), in the ipsilateral neocortex of APP23 mice (Fig. 11). All these results strongly suggest that IL-4/IL-13 reduce chronic inflammation caused by M1-like microglia, and induction of M2-like microglia contribute to the repair of microglial dysfunction, and consequently participate in A β clearance.

3.4 Scope and limitation of single microinjections of IL-4/IL-13 *in vivo* and possible approaches to improve it

In the present study, we used a single microinjection of IL-4/IL-13 into one hemisphere, which allowed direct comparison of the effect on the contralateral side as a control. It is worth noting that this injection actually induced microglial activation in only the ipsilateral side, in which it reduced accumulated A β and consequently improved cognitive deficits in young (4.5-month-old) APP23 mice. In addition, increased expressions of both CD36 and NEP in only the ipsilateral side strongly

suggest that the mechanism that we previously proposed for *in vitro* IL-4-induced A β clearance (Shimizu et al., 2008) operates similarly *in vivo*. Either microinjection of cytokines into both hemispheres or repeating injections may improve cognitive deficits even in older mice, such as those 9 months old, although we have not tested these methods as yet. However, the present method utilizing a surgical microinjection into the brain is difficult to apply as a therapeutic technique, and therefore more sophisticated tactics, such as introduction of agents that stimulate production of IL-4 and IL-13, or microglial activation by either neuronal/glia cells (Nolan et al., 2005) or Th2 cells (Town et al., 2005b) in the brain, may be required.

We previously reported that oral administration of the synthetic retinoid Am80, which increased IL-4 production in the T-cell system (Iwata et al., 2003), reduced brain A β_{42} peptides in APP23 mice (Kawahara et al., 2009). Other compounds such as morphine (Roy et al., 2001), tetrahydrocannabinol (Newton et al., 2009), 1 α ,25-dihydroxyvitamin D3 (Boonstra et al., 2001), atorvastatin (Youssef et al., 2002; Clarke et al., 2008), and glatiramer acetate (Butovsky et al., 2006) also reportedly increase IL-4 production in the T-cell system, and testing them as possible AD therapeutic agents may be worthwhile. However, IL-4 may be involved in the pathogenesis of allergies and brain tumors, such as asthma (Steinke et al., 2001) and gliomas (Rand et al., 2000), respectively, and these possibilities should be remembered during development of IL-4 agonists. Very recently, two papers reported that IL-4, which was expressed by means of adoptive transfer of T cells into IL-4-knockout mice (Derecki et al., 2010) or adenovirus-mediated local delivery in the CNS (Kiyota et al.,

2010), played a critical role in recovery of cognitive impairment and/or attenuation of AD-like pathogenesis, respectively, although their mechanisms differ from ours. Therefore, IL-4 has been accepted as having anti-inflammatory or protective activity in the CNS, in addition to its conventional pathogenic action described above.

In conclusion, IL-4/IL-13-induced clearance of A β , possibly soluble and/or oligomeric A β , via CD36 expression in activated M2-like microglial cells and NEP expression in microglial cells and primarily in neurons, has potential value in therapeutic strategies for AD at early stages. The unique A β clearance mechanisms that we demonstrated here *in vivo* should stimulate additional investigations to discover agents that induce IL-4/IL-13 production in the brain parenchyma or near the blood-brain barrier or blood-cerebrospinal fluid barrier and may encourage development of new anti-inflammatory strategies for the treatment of AD, as well as innovative techniques of mucosal A β vaccination (Weiner et al., 2000).

Acknowledgments: We are grateful to Dr. M. Staufenbiel (Novartis Institutes of BioMedical Research Basel) for his generous gift of APP23 mice, which enabled us to perform this study. We thank H. Hirata, C. Kawahara, K. Nishi, T. Sumi, S. Yokoo, and K. Nagatomo for technical assistance. We also thank Prof. K. Iwasaki (Fukuoka University, Faculty of Pharmaceutical Sciences) for his advice on the behavioral analysis. We are grateful to Prof. T. Gotoh (Kumamoto University, Faculty of

Education) who kindly provided polyclonal anti-arginase I antibody. This work was supported by Grants-in-Aid for Scientific Research of Priority Area “Glia-Neuron Network” 16047224 and 18053019 (to H. N.) and Scientific Research Grants 19390031 (to H. N.) and 17790067 and 21790114 and 23790133 (to K. K.) from the Ministry of Education, Culture, Sports, Science and Technology of Japan.

REFERENCES

- Akiyama H, Barger S, Barnum S, Bradt B, Bauer J, Cole GM, Cooper NR, Eikelenboom P, Emmerling M, Fiebich BL, Finch CE, Frautschy S, Griffin WS, Hampel H, Hull M, Landreth G, Lue L, Mrak R, Mackenzie IR, McGeer PL, O'Banion MK, Pachter J, Pasinetti G, Plata-Salaman C, Rogers J, Rydel R, Shen Y, Streit W, Strommeyer R, Tooyoma I, Van Muiswinkel FL, Veerhuis R, Walker D, Webster S, Wegrzyniak B, Wenk G, Wyss-Coray T (2000) Inflammation and Alzheimer's disease. *Neurobiol Aging* 21:383-421.
- Bales KR, Verina T, Cummins DJ, Du Y, Dodel RC, Saura J, Fishman CE, DeLong CA, Piccardo P, Petegnief V, Ghetti B, Paul SM (1999) Apolipoprotein E is essential for amyloid deposition in the APP^{V717F} transgenic mouse model of Alzheimer's disease. *Proc Natl Acad Sci USA* 96:15233-15238.
- Boonstra A, Barrat FJ, Crain C, Heath VL, Savelkoul HF, O'Garra A (2001) 1 α ,25-Dihydroxyvitamin D3 has a direct effect on naive CD4⁺ T cells to enhance the development of Th2 cells. *J Immunol* 167:4974-4980.
- Butovsky O, Koronyo-Hamaoui M, Kunis G, Ophir E, Landa G, Cohen H, Schwartz M (2006) Glatiramer acetate fights against Alzheimer's disease by inducing dendritic-like microglia expressing insulin-like growth factor 1. *Proc Natl Acad Sci USA* 103:11784-11789.
- Butovsky O, Kunis G, Koronyo-Hamaoui M, Schwartz M (2007) Selective ablation of bone marrow-derived dendritic cells increases amyloid plaques in a mouse

- Alzheimer's disease model. *Eur J Neurosci* 26:413-416.
- Capetillo-Zarate E, Staufenbiel M, Abramowski D, Haass C, Escher A, Stadelmann C, Yamaguchi H, Wiestler OD, Thal DR (2006) Selective vulnerability of different types of commissural neurons for amyloid β -protein-induced neurodegeneration in APP23 mice correlates with dendritic tree morphology. *Brain* 129:2992-3005.
- Cao C, Arendash GW, Dickson A, Mamcarz MB, Lin X, Ethell DW (2009) A β -specific Th2 cells provide cognitive and pathological benefits to Alzheimer's mice without infiltrating the CNS. *Neurobiol Dis.* 34:63-70.
- Chao CC, Molitor TW, Hu S (1993) Neuroprotective role of IL-4 against activated microglia. *J Immunol* 151:1473-1481.
- Clarke RM, Lyons A, O'Connell F, Deighan BF, Barry CE, Anyakoha NG, Nicolaou A, Lynch MA (2008) A pivotal role for interleukin-4 in atorvastatin-associated neuroprotection in rat brain. *J Biol Chem* 283:1808-1817.
- Colton CA, Mott RT, Sharpe H, Xu Q, Van Nostrand WE, Vitek MP (2006) Expression profiles for macrophage alternative activation genes in AD and in mouse models of AD. *J Neuroinflammation* 3:27.
- Cullen KM, Halliday GM (1998) Neurofibrillary degeneration and cell loss in the nucleus basalis in comparison to cortical Alzheimer pathology. *Neurobiol Aging* 19:297-306.
- Dam D V, D'Hooge R, Staufenbiel M, Ginneken CV, Meir FV, De Deyn PP (2003) Age-dependent cognitive decline in the APP23 model precedes amyloid deposition. *Eur J Neurosci* 17:388-396.

- Derecki NC, Cardani AN, Yang CH, Quinlivan KM, Cribfield A, Lynch KR, Kipnis J (2010) Regulation of learning and memory by meningeal immunity: a key role for IL-4. *J Exp Med* 207:1067-1080.
- Duffield JS (2003) The inflammatory macrophage: a story of Jekyll and Hyde. *Clin Sci Lond* 104:27-38.
- El Khoury J, Toft M, Hickman SE, Means TK, Terada K, Geula C, Luster AD (2007) Ccr2 deficiency impairs microglial accumulation and accelerates progression of Alzheimer-like disease. *Nat Med* 13:432-438.
- Goerdt S, Orfanos CE (1999) Other functions, other genes: alternative activation of antigen-presenting cells. *Immunity* 10:137-142.
- Hardy J, Selkoe DJ (2002) The amyloid hypothesis of Alzheimer's disease: progress and problems on the road to therapeutics. *Science* 297:353-356.
- Hickman SE, Allison EK, El Khoury J (2008) Microglial dysfunction and defective β -amyloid clearance pathways in aging Alzheimer's disease mice. *J Neurosci* 28:8354-8360.
- Hoshi M, Sato M, Matsumoto S, Noguchi A, Yasutake K, Yoshida N, Sato K (2003) Spherical aggregates of β -amyloid (amylospheroid) show high neurotoxicity and activate tau protein kinase I/glycogen synthase kinase-3 β . *Proc Natl Acad Sci U S A* 100:6370-6375.
- Iwata M, Eshima Y, Kagechika H (2003) Retinoic acids exert direct effects on T cells to suppress T_H1 development and enhance T_H2 development via retinoic acid receptors. *Int Immunol* 15:1017-1025.

- Iwatsubo T, Odaka A, Suzuki N, Mizusawa H, Nukina N, Ihara Y (1994) Visualization of A β ₄₂₍₄₃₎ and A β ₄₀ in senile plaques with end-specific A β monoclonals: evidence that an initially deposited species is A β ₄₂₍₄₃₎. *Neuron* 13:45-53.
- Kawahara K, Nishi K, Suenobu M, Ohtsuka H, Maeda A, Nagatomo K, Kuniyasu A, Staufenbiel M, Nakagomi M, Shudo K, Nakayama H (2009) Oral administration of synthetic retinoid Am80 (Tamibarotene) decreases brain β -amyloid peptides in APP23 mice. *Biol Pharm Bull* 32:1307-1309.
- Kayed R, Head E, Thompson JL, McIntire TM, Milton SC, Cotman CW, Glabe CG (2003) Common structure of soluble amyloid oligomers implies common mechanism of pathogenesis. *Science* 300:486-489.
- Kim J, Basak JM, Holtzman DM (2009) The role of apolipoprotein E in Alzheimer's disease. *Neuron* 63:287-303.
- Kiyota T, Okuyama S, Swan RJ, Jacobsen MT, Gendelman HE, Ikezu T (2010) CNS expression of anti-inflammatory cytokine interleukin-4 attenuates Alzheimer's disease-like pathogenesis in APP+PS1 bigenic mice. *FASEB J* 24:3093-3102.
- Koenigsknecht-Talboo J, Landreth GE (2005) Microglial phagocytosis induced by fibrillar β -amyloid and IgGs are differentially regulated by proinflammatory cytokines. *J Neurosci* 25:8240-8249.
- Mantovani A, Sozzani S, Locati M, Allavena P, Sica A (2002) Macrophage polarization: tumor-associated macrophages as a paradigm for polarized M2 mononuclear phagocytes. *Trends Immunol* 23:549-555.
- Matsunaga W, Shirokawa T, Isobe K (2003) Specific uptake of A β 1-40 in rat brain

- occurs in astrocyte, but not in microglia. *Neurosci Lett* 342:129-131.
- McGeer PL, McGeer EG (2001) Inflammation, autotoxicity and Alzheimer's disease. *Neurobiol Aging* 22:799-809.
- Mohamed A, Posse de Chaves E (2011) A β internalization by neurons and glia. *Int J Alzheimers Dis* 2011, doi: 10.4061/2011/127984.
- Morris R (1984) Developments of a water-maze procedure for studying spatial learning in the rat. *J Neurosci Methods* 11:47-60.
- Newton CA, Chou PJ, Perkins I, Klein TW (2009) CB₁ and CB₂ cannabinoid receptors mediate different aspects of delta-9-tetrahydrocannabinol (THC)-induced T helper cell shift following immune activation by *Legionella pneumophila* infection. *J Neuroimmune Pharmacol.* 4:92-102.
- Nolan Y, Maher FO, Martin DS, Clarke RM, Brady MT, Bolton AE, Mills KH, Lynch MA (2005) Role of interleukin-4 in regulation of age-related inflammatory changes in the hippocampus. *J Biol Chem* 280:9354-9362.
- Oddo S, Billings L, Kesslak JP, Cribbs DH, LaFerla FM (2004) A β immunotherapy leads to clearance of early, but not late, hyperphosphorylated tau aggregates via the proteasome. *Neuron* 43:321-332.
- Oddo S, Caccamo A, Smith IF, Green KN, LaFerla FM (2006) A dynamic relationship between intracellular and extracellular pools of A β . *Am J Pathol* 168:184-194.
- Paxinos G, Franklin KB (2004) *The mouse brain in stereotaxic coordinates*, 2nd ed. Compact ed. San Diego: Academic Press.
- Rand RW, Kreitman RJ, Patronas N, Varricchio F, Pastan I, Puri RK (2000)

- Intratumoral administration of recombinant circularly permuted interleukin-4-Pseudomonas exotoxin in patients with high-grade glioma. *Clin Cancer Res* 6:2157-2165.
- Roder S, Danober L, Pozza MF, Lingenhoehl K, Wiederhold KH, Olpe HR (2003) Electrophysiological studies on the hippocampus and prefrontal cortex assessing the effects of amyloidosis in amyloid precursor protein 23 transgenic mice. *Neuroscience* 120:705-720.
- Roy S, Balasubramanian S, Sumandeeep S, Charboneau R, Wang J, Melnyk D, Beilman GJ, Vatassery R, Barke RA (2001) Morphine directs T cells toward T_{H2} differentiation. *Surgery* 130:304-309.
- Saito T, Iwata N, Tsubuki S, Takaki Y, Takano J, Huang SM, Suemoto T, Higuchi M, Saido TC (2005) Somatostatin regulates brain amyloid β peptide A β ₄₂ through modulation of proteolytic degradation. *Nat Med* 11:434-439.
- Schenk D, Barbour R, Dunn W, Gordon G, Grajeda H, Guido T, Hu K, Huang J, Johnson-Wood K, Khan K, Kholodenko D, Lee M, Liao Z, Lieberburg I, Motter R, Mutter L, Soriano F, Shopp G, Vasquez N, Vandevent C, Walker S, Wogulis M, Yednock T, Games D, Seubert P (1999) Immunization with amyloid- β attenuates Alzheimer-disease-like pathology in the PDAPP mouse. *Nature* 400:173-177.
- Shaw KN, Commins S, O'Mara SM (2001) Lipopolysaccharide causes deficits in spatial learning in the watermaze but not in BDNF expression in the rat dentate gyrus. *Behav Brain Res* 124:47-54.
- Shimizu E, Kawahara K, Kajizono M, Sawada M, Nakayama H (2008) IL-4-induced

- selective clearance of oligomeric β -amyloid peptide₁₋₄₂ by rat primary type 2 microglia. *J Immunol* 181:6503-6513.
- Sonoki T, Nagasaki A, Gotoh T, Takiguchi M, Takeya M, Matsuzaki H, Mori M. (1997) Coinduction of nitric-oxide synthase and arginase I in cultured rat peritoneal macrophages and rat tissues in vivo by lipopolysaccharide. *J Biol Chem* 272:3689-3693.
- Steinke JW, Borish L (2001) Th2 cytokines and asthma. Interleukin-4: its role in the pathogenesis of asthma, and targeting it for asthma treatment with interleukin-4 receptor antagonists. *Respir Res* 2:66-70.
- Sturchler-Pierrat C, Abramowski D, Duke M, Wiederhold KH, Mistl C, Rothacher S, Ledermann B, Bürki K, Frey P, Paganetti PA, Waridel C, Calhoun ME, Jucker M, Probst A, Staufenbiel M, Sommer B (1997) Two amyloid precursor protein transgenic mouse models with Alzheimer disease-like pathology. *Proc Natl Acad Sci U S A* 94:13287-13292.
- Suzumura A, Sawada M, Itoh Y, Marunouchi T (1994) Interleukin-4 induces proliferation and activation of microglia but suppresses their induction of class II major histocompatibility complex antigen expression. *J Neuroimmunol* 53:209-218.
- Szczepanik AM, Funes S, Petko W, Ringheim GE (2001) IL-4, IL-10 and IL-13 modulate A β ₁₋₄₂-induced cytokine and chemokine production in primary murine microglia and a human monocyte cell line. *J Neuroimmunol* 113:49-62.
- Tampellini D, Rahman N, Gallo EF, Huang Z, Dumont M, Capetillo-Zarate E, Ma T,

- Zheng R, Lu B, Nanus DM, Lin MT, Gouras GK (2009) Synaptic activity reduces intraneuronal A β , promotes APP transport to synapses, and protects against A β -related synaptic alterations. *J Neurosci* 29:9704-9713.
- Town T, Nikolic V, Tan J (2005a) The microglial "activation" continuum: from innate to adaptive responses. *J Neuroinflammation* 2:24.
- Town T, Tan J, Flavell RA, Mullan M. (2005b) T-cells in Alzheimer's disease. *Neuromolecular Med.* 7:255-264.
- Town T, Vendrame M, Patel A, Poetter D, DelleDonne A, Mori T, Smeed R, Crawford F, Klein T, Tan J, Mullan M (2002) Reduced Th1 and enhanced Th2 immunity after immunization with Alzheimer's β -amyloid₁₋₄₂. *J Neuroimmunol* 132:49-59.
- Vorhees CV, Williams MT (2006) Morris water maze: procedures for assessing spatial and related forms of learning and memory. *Nat Protoc.* 1:848-858.
- Weiner HL, Lemere CA, Maron R, Spooner ET, Grenfell TJ, Mori C, Issazadeh S, Hancock WW, Selkoe DJ (2000) Nasal administration of amyloid- β peptide decreases cerebral amyloid burden in a mouse model of Alzheimer's disease. *Ann Neurol* 48:567-579.
- Winkler J, Suhr ST, Gage FH, Thal LJ, Fisher LJ (1995) Essential role of neocortical acetylcholine in spatial memory. *Nature* 375:484-487.
- Yamamoto M, Kiyota T, Walsh SM, Liu J, Kipnis J, Ikezu T (2008) Cytokine-mediated inhibition of fibrillar amyloid- β peptide degradation by human mononuclear phagocytes. *J Immunol* 181:3877-3886.
- Yang AJ, Chandswangbhuvana D, Shu T, Henschen A, Glabe CG (1999) Intracellular

accumulation of insoluble, newly synthesized A β _n-42 in amyloid precursor protein-transfected cells that have been treated with A β ₁₋₄₂. *J Biol Chem* 274:20650-20656.

Youssef S, Stüve O, Patarroyo JC, Ruiz PJ, Radosevich JL, Hur EM, Bravo M, Mitchell DJ, Sobel RA, Steinman L, Zamvil SS (2002) The HMG-CoA reductase inhibitor, atorvastatin, promotes a Th2 bias and reverses paralysis in central nervous system autoimmune disease. *Nature* 420:39-40.

Zelcer N, Khanlou N, Clare R, Jiang Q, Reed-Geaghan EG, Landreth GE, Vinters HV, Tontonoz P (2007) Attenuation of neuroinflammation and Alzheimer's disease pathology by liver x receptors. *Proc Natl Acad Sci U S A* 104:10601-10606.

(FIGURE LEGENDS)

Fig. 1. Intracerebral microinjection of IL-4/IL-13 reversed deficits in spatial learning and memory in 4.5-month-old APP23 mice. Spatial learning and memory were evaluated by means of the MWM test from day 4 to day 7 after microinjection of IL-4/IL-13 or saline into the left neocortex. (A) Mice were trained to swim to the hidden platform for 4 consecutive days. Each point represents the mean latency to find the escape platform of three to five trials per day \pm SEM for the indicated group. Statistical differences were calculated by using the two-way ANOVA. $***P<0.001$, for the difference between IL-4/IL-13-injected APP23 mice and saline-injected mice. (B, C) Test of memory in the MWM probe trial without the use of the platform. (a) APP23 mice. (b) WT mice. Measures included (B) the percent time searching each quadrant and (C) the number of crossings over the training annulus, which was $3.1 \times$ the size of the target platform, during a probe trial (a 100-s session). Error bars represent means \pm SEM. Statistical differences were calculated by means of Student's *t*-test and one-way ANOVA, followed by post hoc Dunnett's multiple comparison test. $**P<0.01$ by Student's *t*-test. $###P<0.001$ and $^{\#}P<0.05$ by Dunnett's multiple comparison test, relative to other quadrants.

Fig. 2. Intracerebral microinjection of IL-4/IL-13 had no effect on deficits in spatial learning and memory in 9-month-old APP23 mice. (A) Acquisition of spatial learning in the MWM hidden-platform task. Ordinate shows the latency to find a hidden escape

platform. Error bars represent means \pm SEM. (B, C) Test of memory in the MWM probe trial without the use of the platform. (a) APP23 mice. (b) WT mice. Measures included (B) the percent time searching each quadrant and (C) the number of crossings over the training annulus during a probe trial (a 100-s session). Error bars represent means \pm SEM. Statistical differences were calculated by using Student's *t*-test and one-way ANOVA, followed by post hoc Dunnett's multiple comparison test. *** $P < 0.001$ and ** $P < 0.01$ by Student's *t*-test. ### $P < 0.001$ by Dunnett's multiple comparison test, relative to other quadrants.

Fig. 3. Intracerebral microinjection of IL-4/IL-13 reduced total A β levels in the brain. After the behavioral study for 4 days (therefore, at 7 days after the microinjection), brains were harvested and immunohistochemistry was used to analyze the total A β levels in each brain. (A) Coronal sections of neocortex from IL-4/IL-13-injected or saline-injected 4.5-month-old APP23 mice were stained with b4G8 antibody (i.e., anti-A β_{17-24} antibody reactive to any A β form, including A β_{1-42} , A β_{1-40} , and full-length APP). Scale bar=200 μ m. (B, C) Quantitative assessment of the change [given as an ipsilateral/contralateral ratio (in B), or as an immunostaining value (in C)] in b4G8⁺ A β levels in the neocortex of IL-4/IL-13- or saline-injected APP23 mice at ages of 4.5 months (a) and 9 months (b). Error bars represent means \pm SEM ($n=14$ in a, $n=7$ in b). ** $P < 0.01$ and * $P < 0.05$ by Student's *t*-test. # $P < 0.05$ for the ipsilateral side of IL-4/IL-13-injected mice vs. that of other groups.

Fig. 4. Improvement in the memory of IL-4/IL-13-injected APP23 mice was correlated with decreased intraneuronal A β_{40} peptide levels in the brain. After the behavioral study (brains harvested 7 days after the microinjection), immunohistochemistry was used to analyze the A β_{40} levels in each brain. (A, C) Continuous coronal sections shown in Fig. 3 were stained with BA27 antibody (anti-A β_{x-40}). (A) Results for 4.5-month-old APP23 mice. (C) Results for 9-month-old APP23 mice. Scale bars=50 μ m. (B, D) Quantitative assessment of the change in BA27⁺ A β_{40} levels in the neocortex of IL-4/IL-13-injected or saline-injected APP23 mice at ages of 4.5 months (B) and 9 months (D). Error bars represent means \pm SEM ($n=14-18$ (B) and $n=5-6$ (D) for each group). [#] $P<0.05$ for the ipsilateral side of IL-4/IL-13-injected mice vs. that of other groups.

Fig. 5. A β_{42} and A β_{40} levels were significantly decreased in the brains of APP23 mice injected with IL-4/IL-13 compared with the saline-injected group. Seven days after intracerebral injection of IL-4/IL-13 into 4.5-month-old APP23 mice, the ipsilateral and contralateral cerebral cortices were dissected. Guanidine-soluble A β_{42} (A) and A β_{40} (B) levels were determined by using sandwich ELISA. Error bars represent means \pm SEM ($n=15$ (A) and $n=6$ (B) for the IL-4/IL-13-injected group, $n=16$ (A) and $n=7$ (B)). [#] $P<0.05$ for the ipsilateral side of IL-4/IL-13-injected mice vs. that of other groups. (C) Scatterplot and Pearson correlation analyses were used to determine the relationship between the A β_{42} values in the ipsilateral side and the percentage of time spent in the target quadrant, for IL-4/IL-13- or saline-injected APP23 mice of 4.5-month-old. (D)

Endogenous A β_{42} levels decreased significantly in the brains of 9-month-old WT mice by injection of IL-4/IL-13 compared with the saline-injected group. Seven days after intracerebral injection of IL-4/IL-13, the ipsilateral and contralateral cerebral cortices were dissected. TBS-soluble A β_{42} levels were determined by using a highly sensitive sandwich ELISA. Error bars represent means \pm SEM ($n=3$ for the IL-4/IL-13-injected group, and $n=4$ for the saline-injected group). * $P=0.038$ by Student's t -test. ^{##} $P<0.01$ by Dunnett's multiple comparison test vs. the IL-4/IL-13-injected ipsilateral side.

Fig. 6. IL-4/IL-13 microinjection activated microglial cells. (A) Immunoreactivity for Iba1 in the ipsilateral neocortex (Ipsi) surrounding the injection site is compared with that in the contralateral side (Contra) at various times after the IL-4/IL-13 microinjection. Scale bars=50 μm . (B) Immunoreactivity for Iba1 in the ipsilateral neocortex surrounding the injection site is compared with that in the contralateral side at 2 days after the microinjection of IL-4/IL-13 or saline. Scale bar=50 μm . (C) The number of Iba1⁺ microglial cells was counted in an area of $390 \times 510 \mu\text{m}^2$ (around the injection site). Data are means \pm SEM ($n=4-8$ for each group). ^{###} $P<0.001$ for the ipsilateral neocortex at 2 days after the IL-4/IL-13 injection vs. that of all other groups.

Fig. 7. IL-4/IL-13 microinjection induced CD36 and NEP. Immunoreactivity for CD36 (A) and NEP (B) in the ipsilateral neocortex surrounding the injection site and in the contralateral side at 2 days after the IL-4/IL-13 microinjection is shown. Scale bars=50 μm .

Fig. 8. Activated microglial cells manifested an increased expression of CD36 and a slight increase of NEP after microinjection of IL-4/IL-13. Double immunofluorescent staining with anti-CD36 and anti-Iba1 (A) and with anti-NEP and anti-Iba1 (B) was performed at 2 days after IL-4/IL-13 injection, and the results of the ipsilateral neocortex surrounding the injection site and those of the contralateral side are shown. The arrows point to CD36⁺ cells (A) and NEP⁺ cells (B). Scale bars=100 μ m.

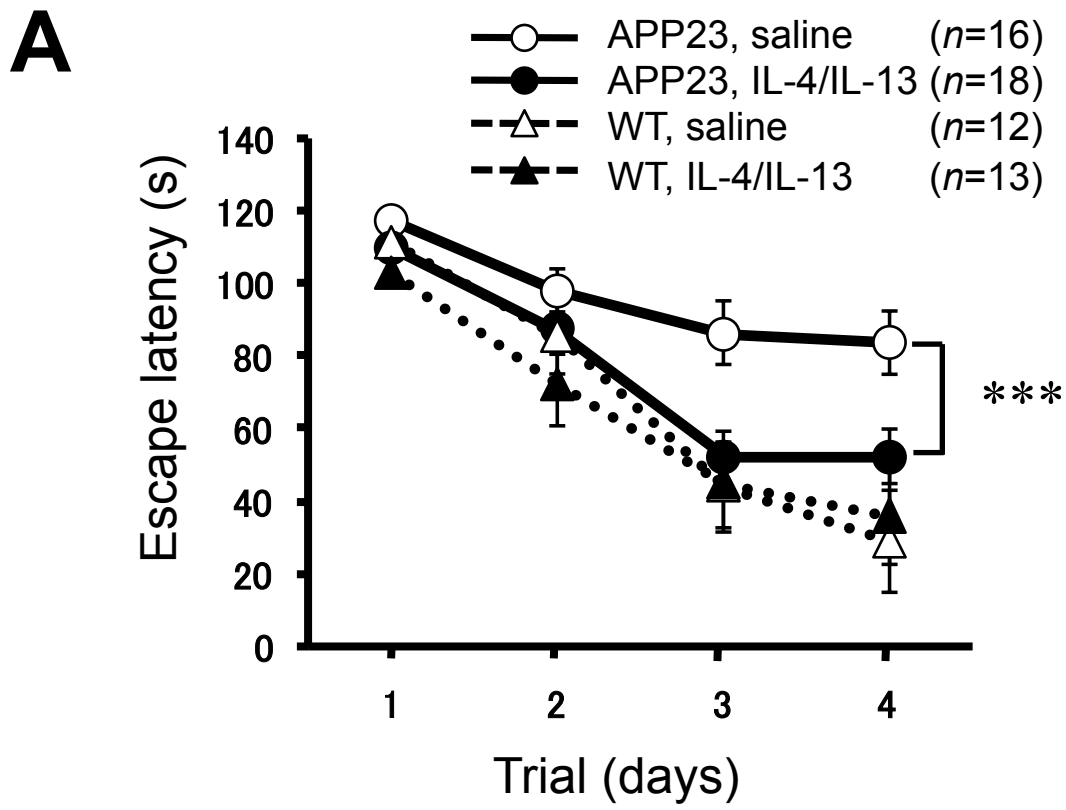
Fig. 9. NEP and IL-4R α were mainly induced in synaptophysin-positive neurons and CD68⁺ microglial cells, respectively, in the ipsilateral side after IL-4/IL-13 injection. (A) Double immunofluorescent staining with anti-NEP and anti-synaptophysin was performed at 2 days after IL-4/IL-13 injection, and results of the ipsilateral neocortex surrounding the injection site and those of the contralateral side are shown. Scale bar=50 μ m. (B) Double immunofluorescent staining with anti-IL-4R α and anti-CD68 was performed at 2 days after IL-4/IL-13 injection, and results of the ipsilateral neocortex surrounding the injection site and those of the contralateral side are shown. Scale bar=50 μ m.

Fig. 10. IL-4/IL-13 microinjection induced alternative microglial activation. Two days after IL-4/IL-13 injection, immunoreactivity for arginase I (A), Ym1 (B), and CD163 (C) in the ipsilateral neocortex surrounding the injection site and in the contralateral side is shown. Double immunofluorescent staining with anti-CD36 and anti-arginase I

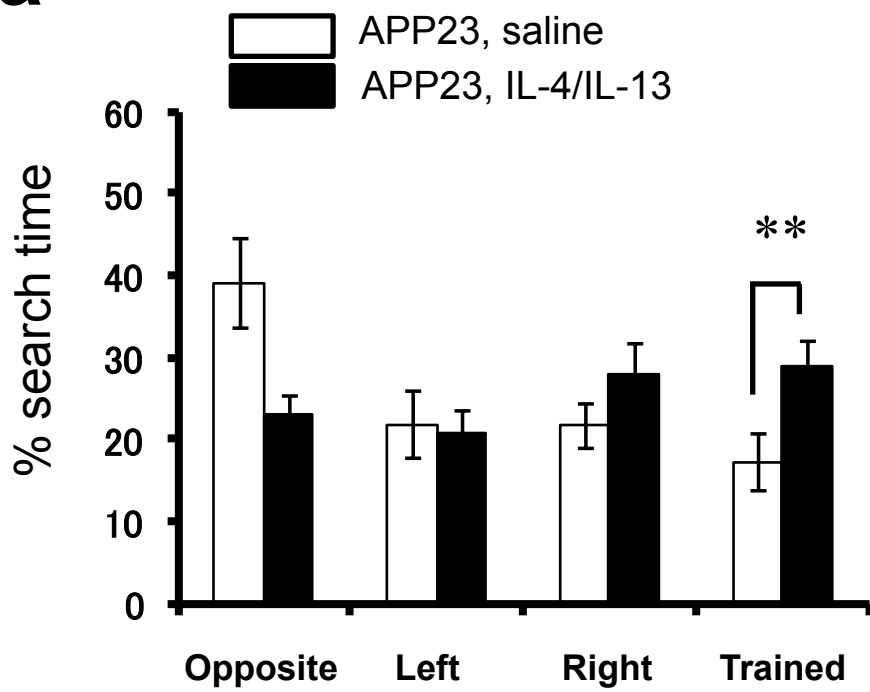
(D) and with anti-CD36 and anti-Ym1 (E) was also performed using similar sections of the ipsilateral neocortex. Scale bars=50 μ m.

Fig. 11. IL-4/IL-13 microinjection reduced the TNF- α level in the ipsilateral neocortex of APP23 mice. (A) Seven days after intracerebral injection of IL-4/IL-13 into 4.5-month-old APP23 mice, the ipsilateral and contralateral cerebral cortices were dissected. PBS-soluble fractions were determined by using sandwich ELISA. Error bars represent means \pm SEM ($n=4$ for each group). [#] $P<0.05$ by Dunnett's multiple comparison test versus the IL-4/IL-13-injected ipsilateral side. (B) Scatterplot and Pearson correlation analyses were used to determine the relationship between the TNF- α values in the ipsilateral side and the percentage of time spent in the target quadrant, for IL-4/IL-13-injected or saline-injected APP23 mice.

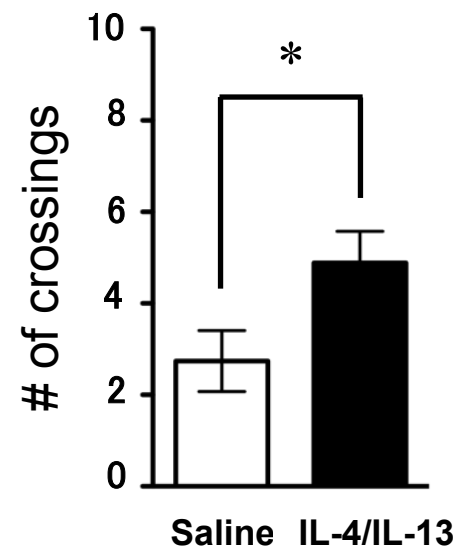
Fig. 1



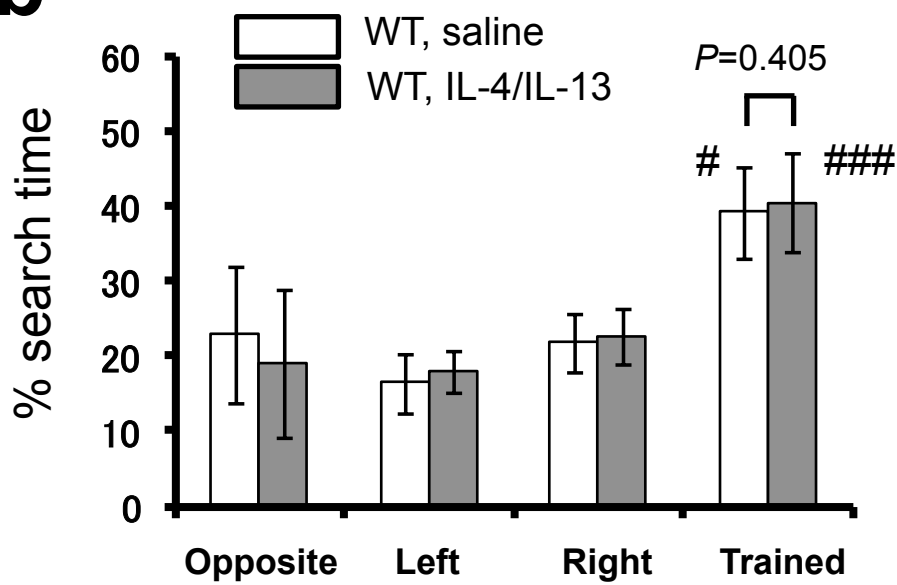
Ba



Ca



Bb



Cb

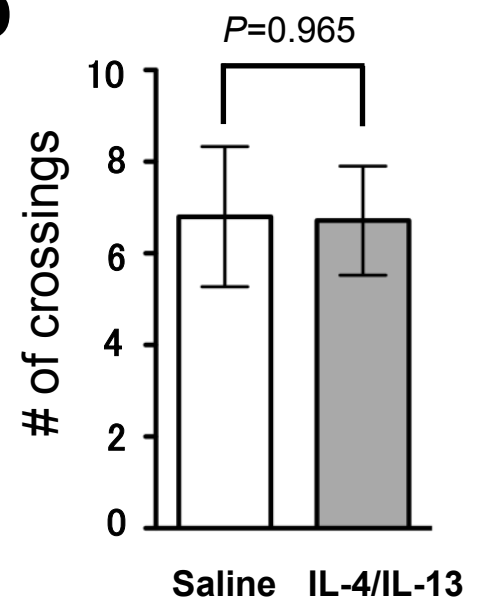
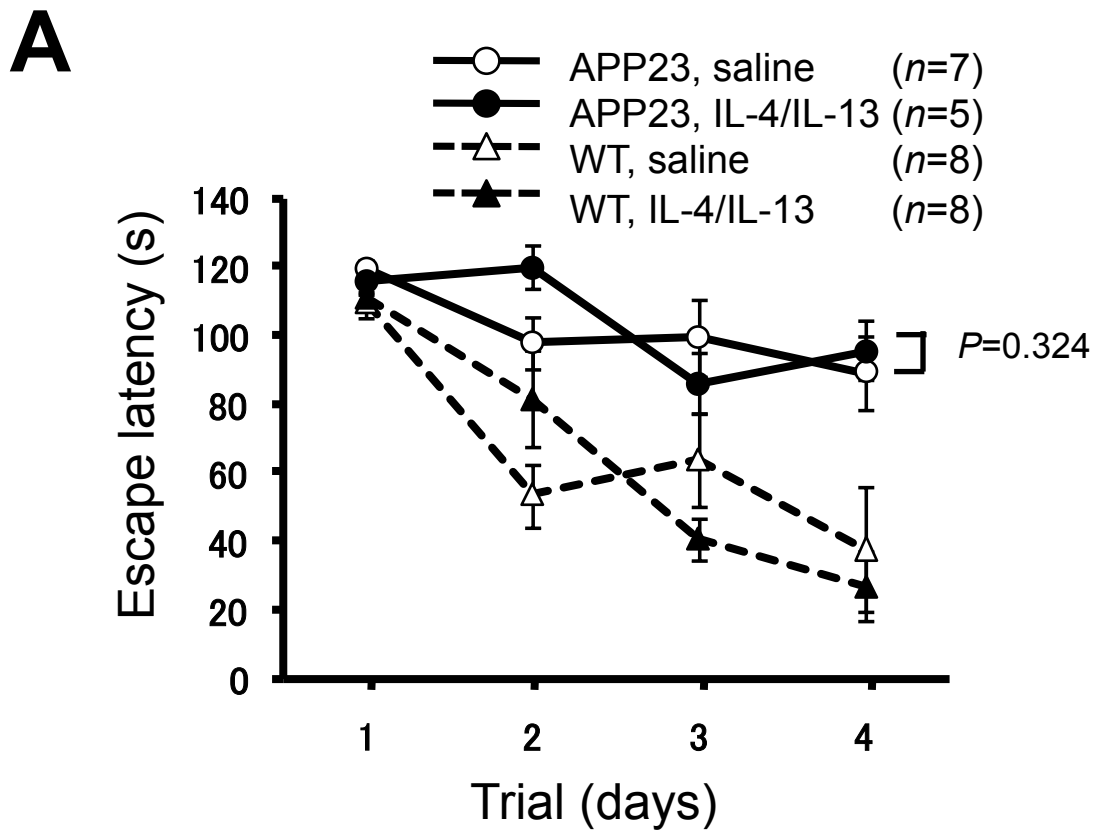
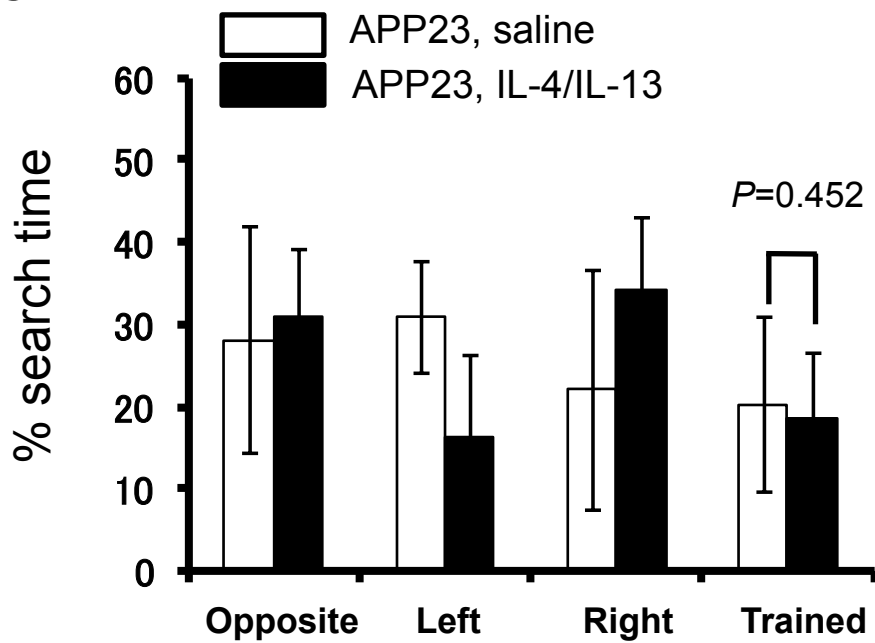


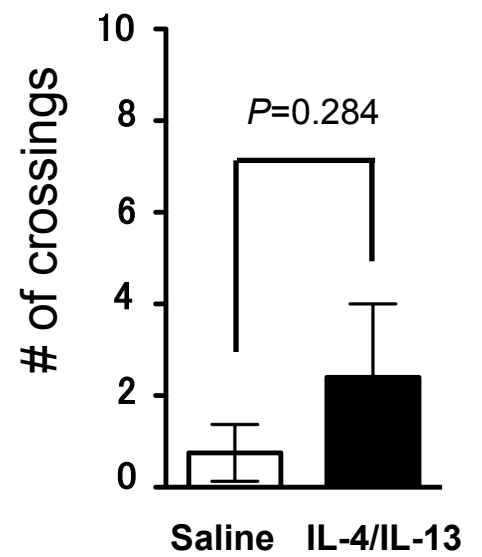
Fig. 2



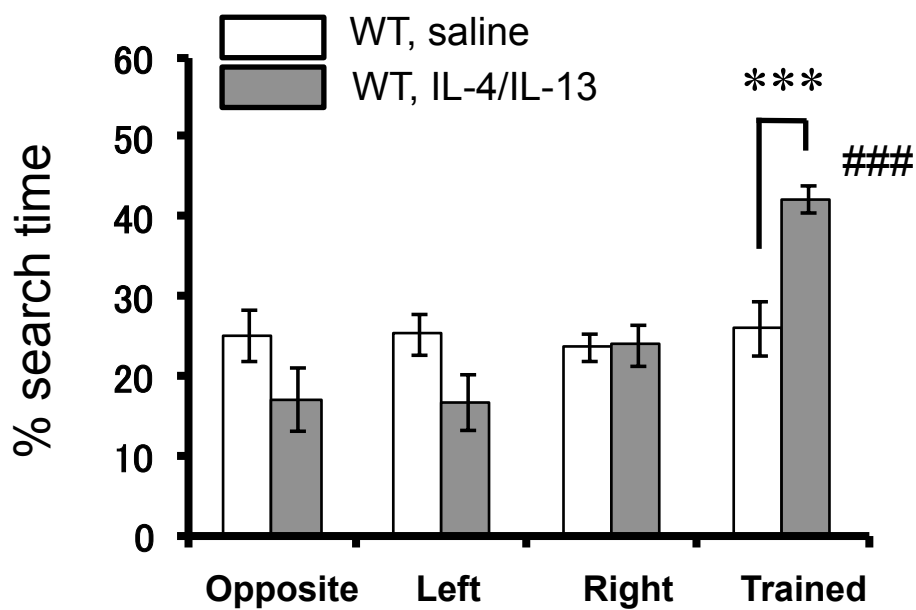
Ba



Ca



Bb



Cb

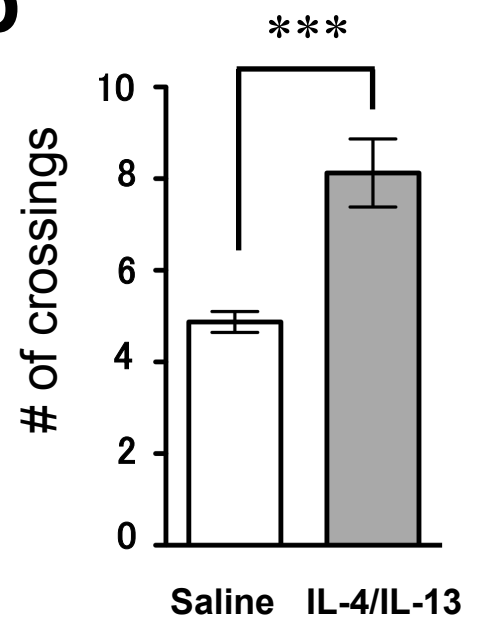


Fig. 3

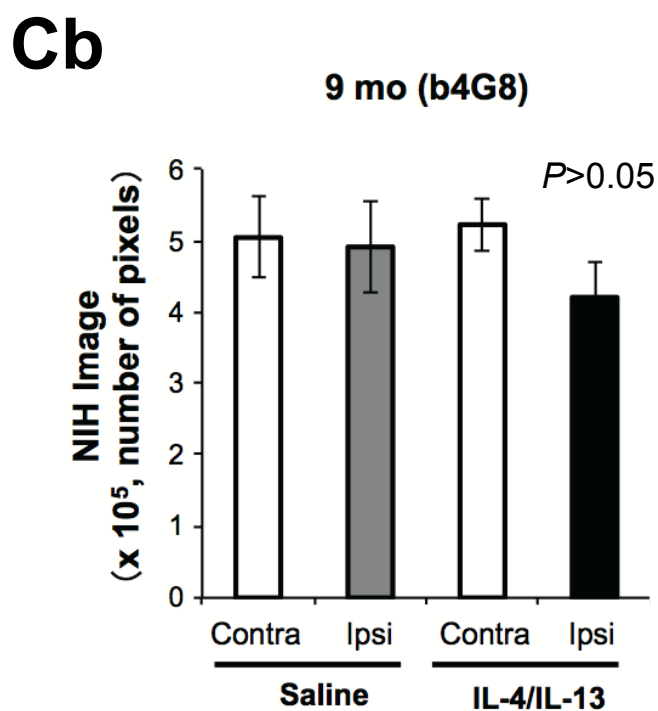
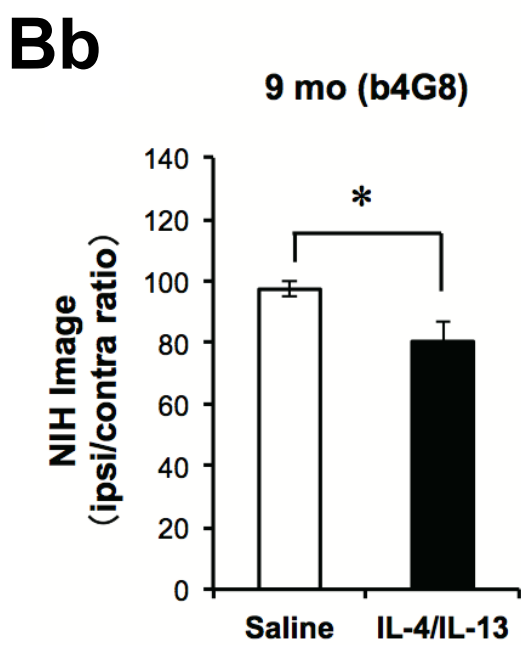
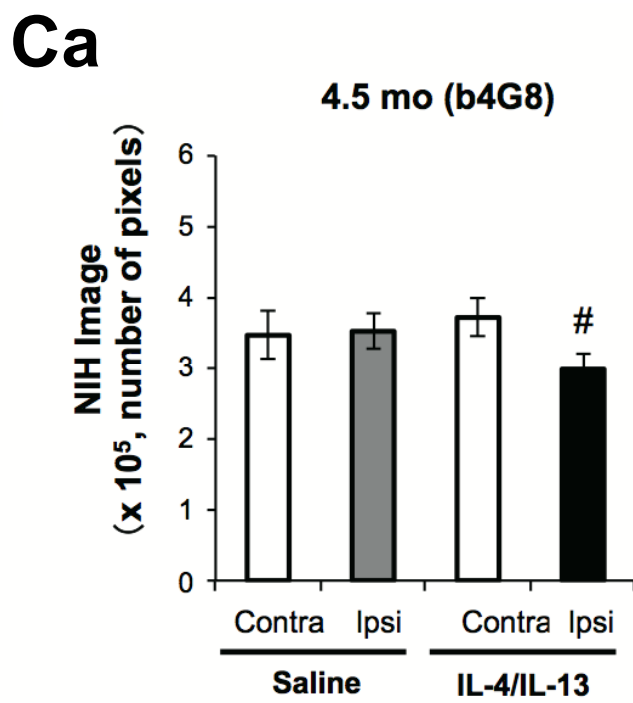
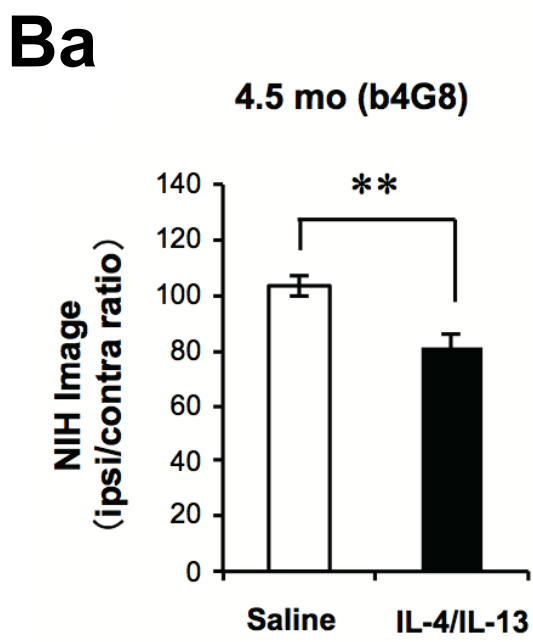
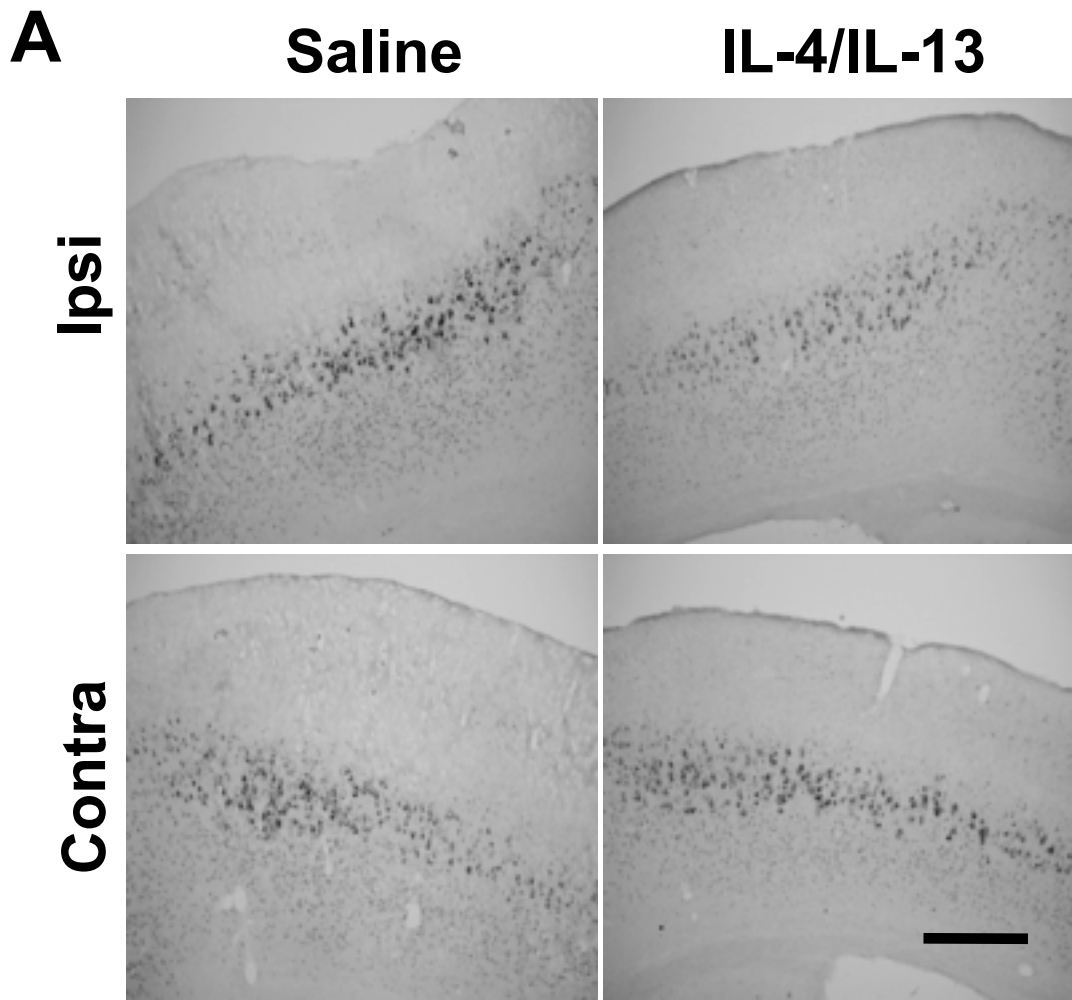


Fig. 4

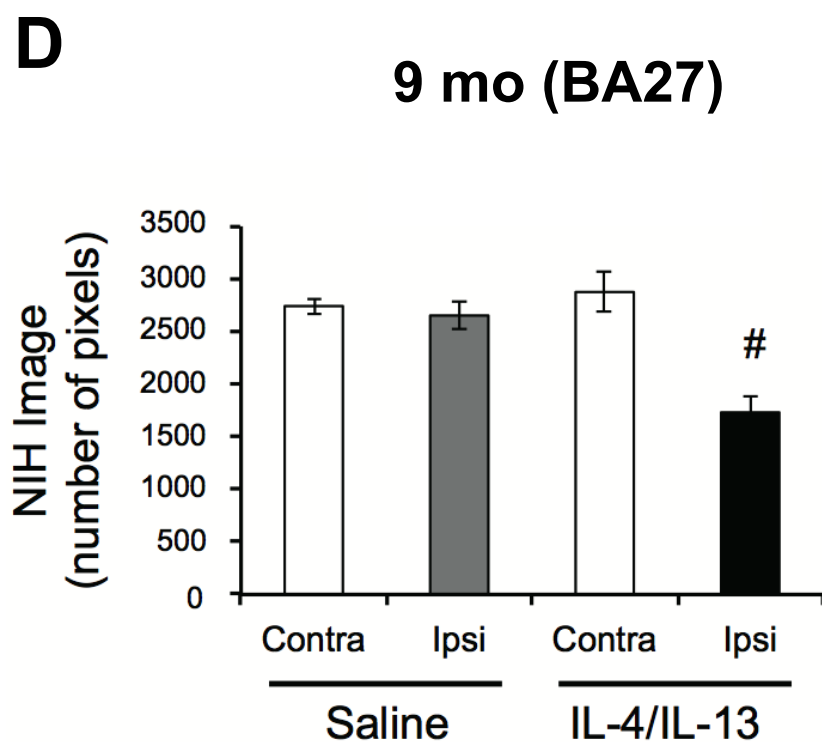
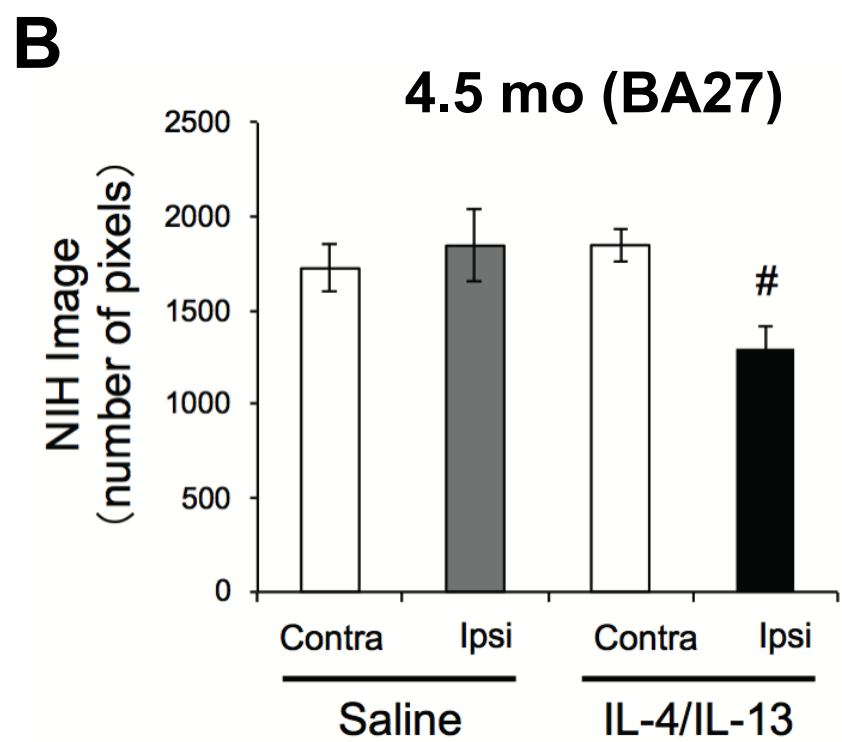
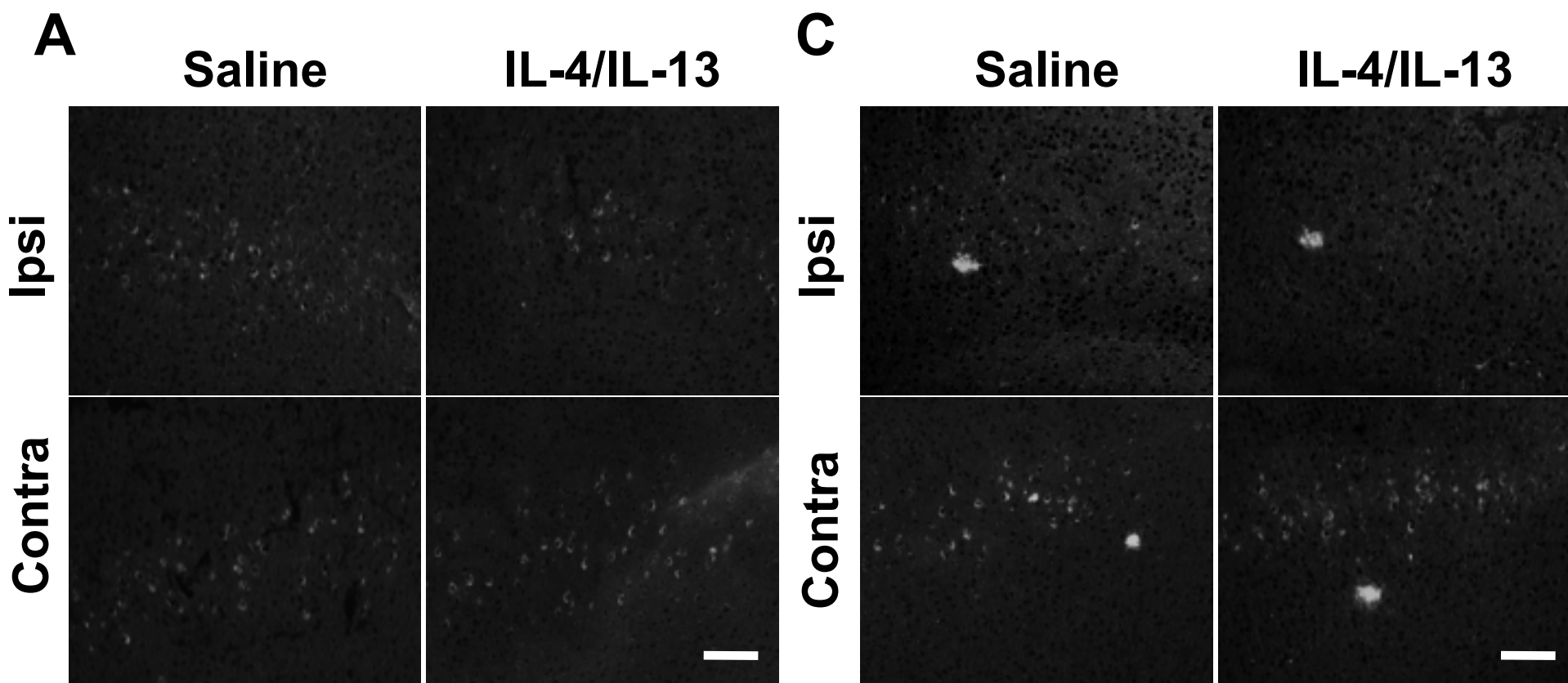


Fig. 5

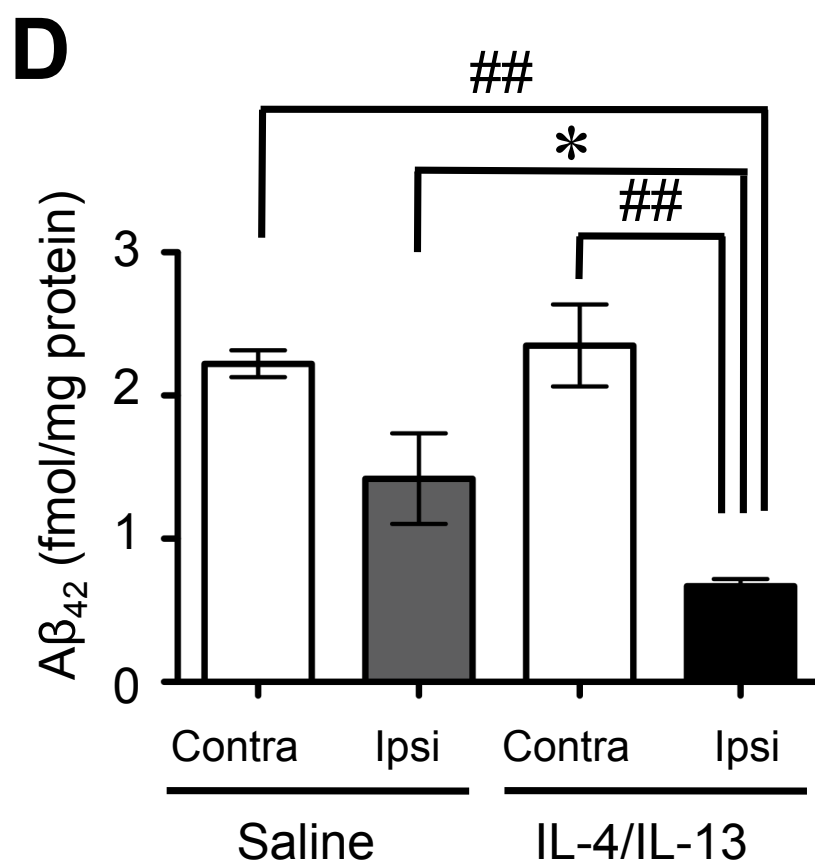
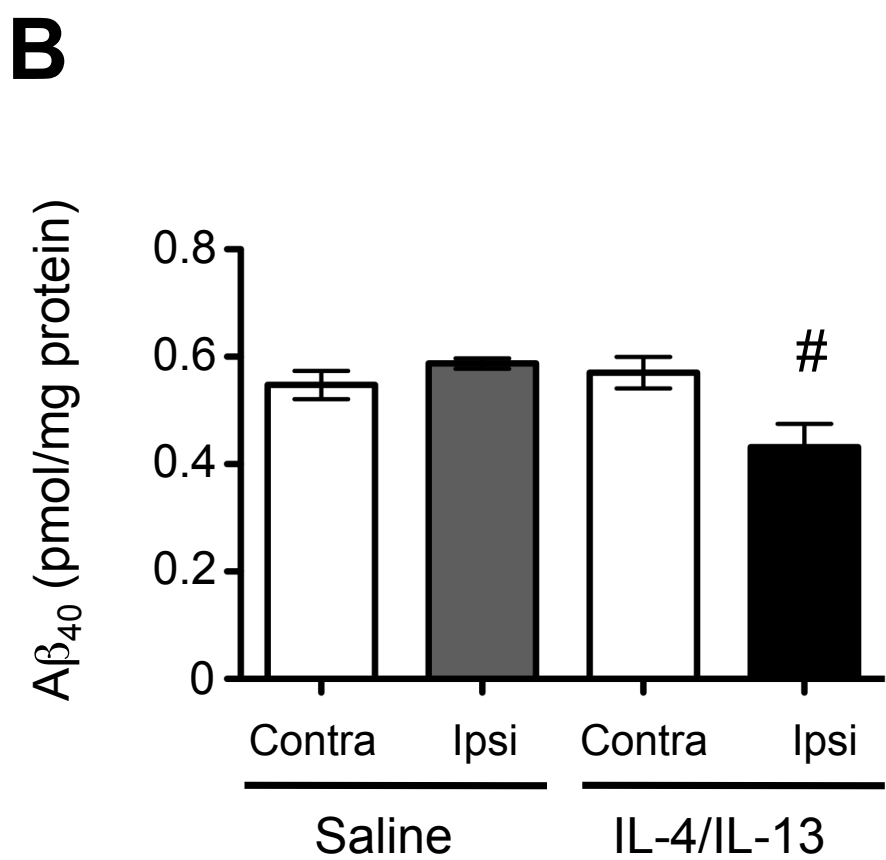
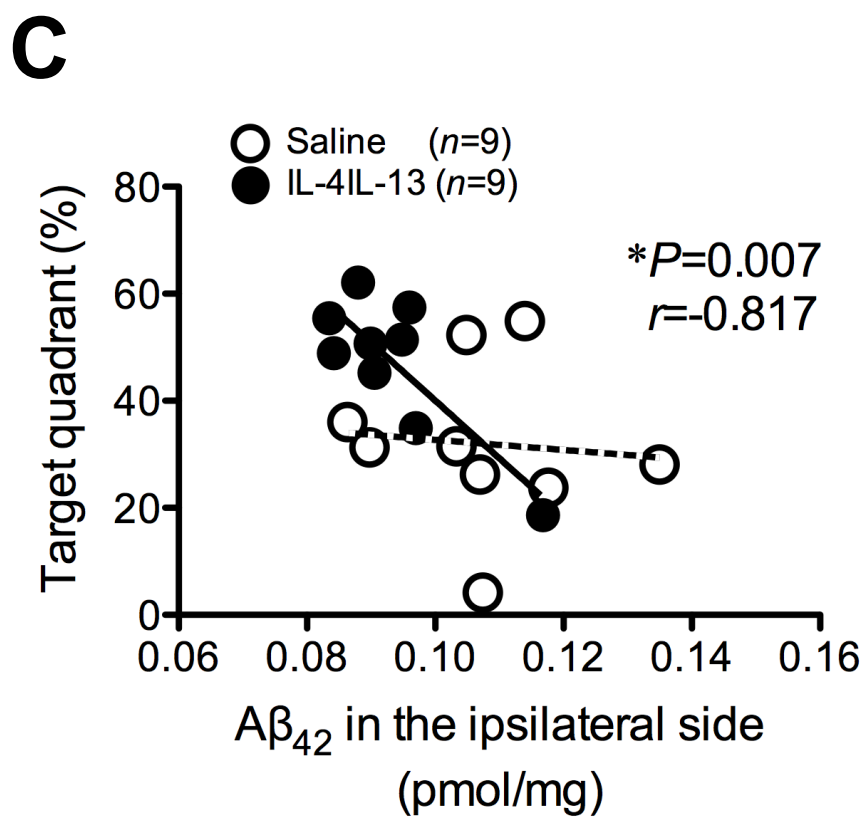
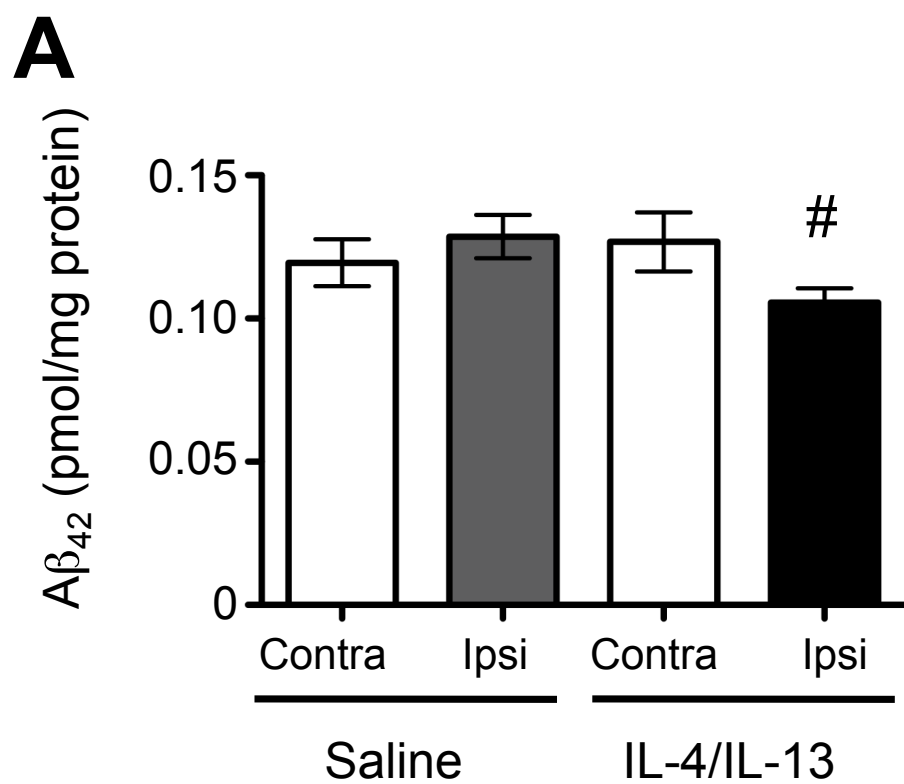


Fig. 6

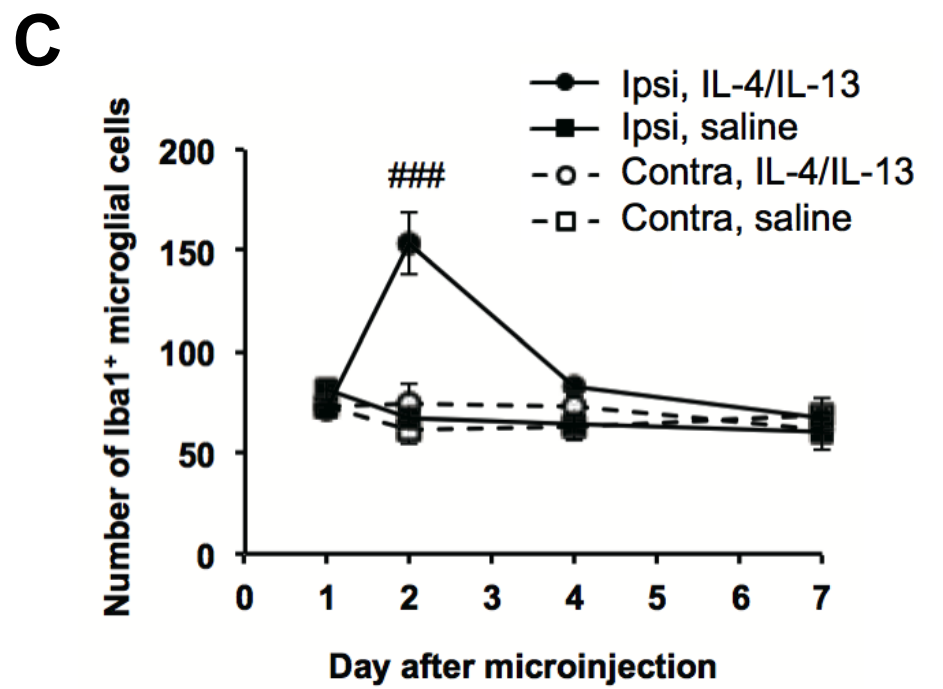
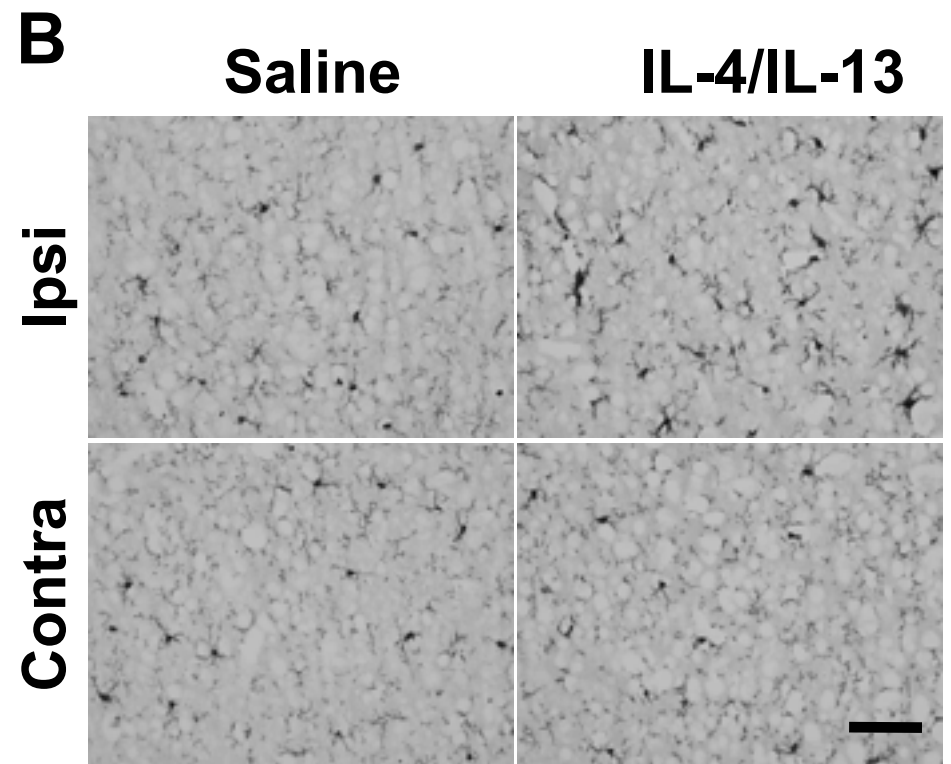
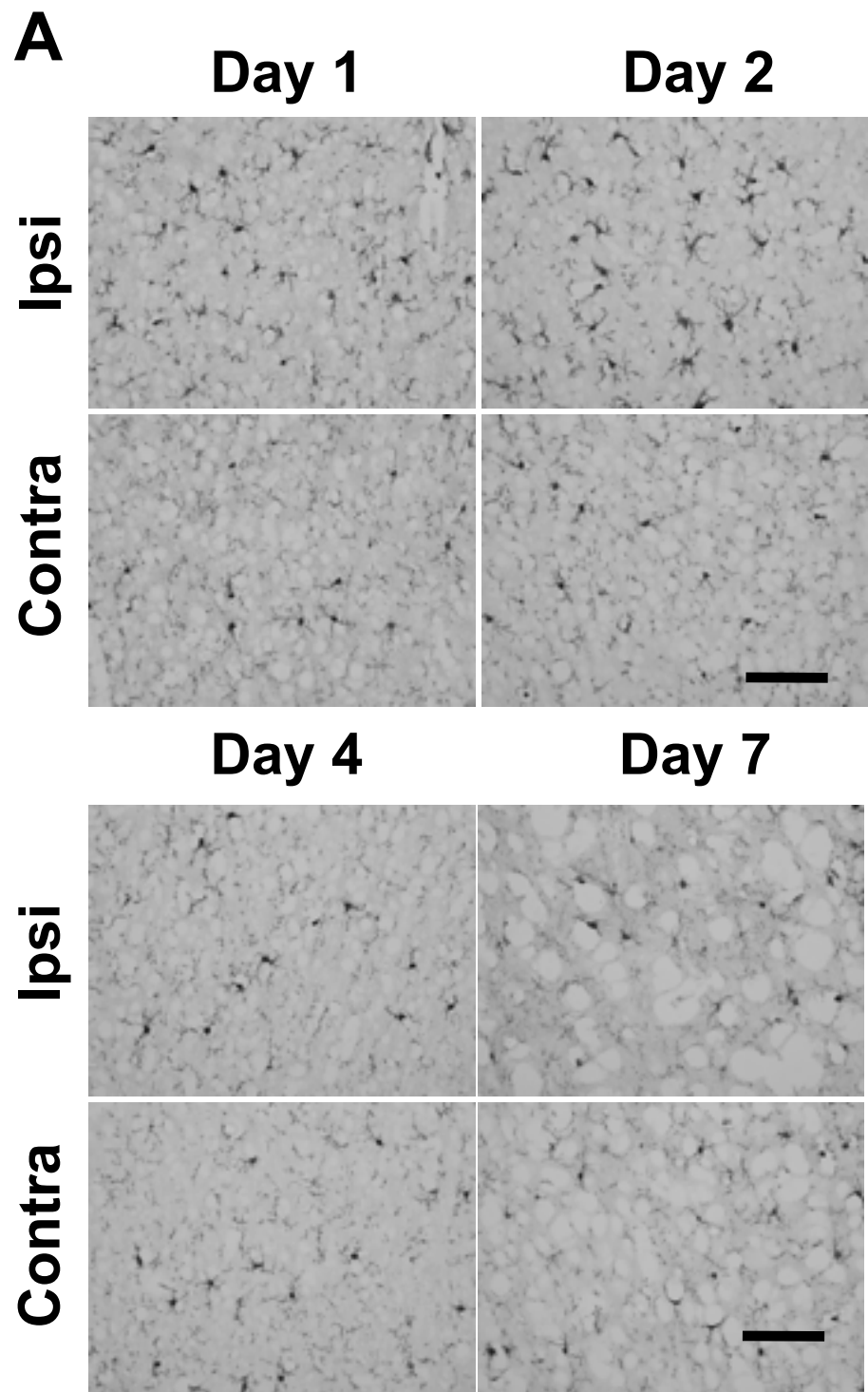
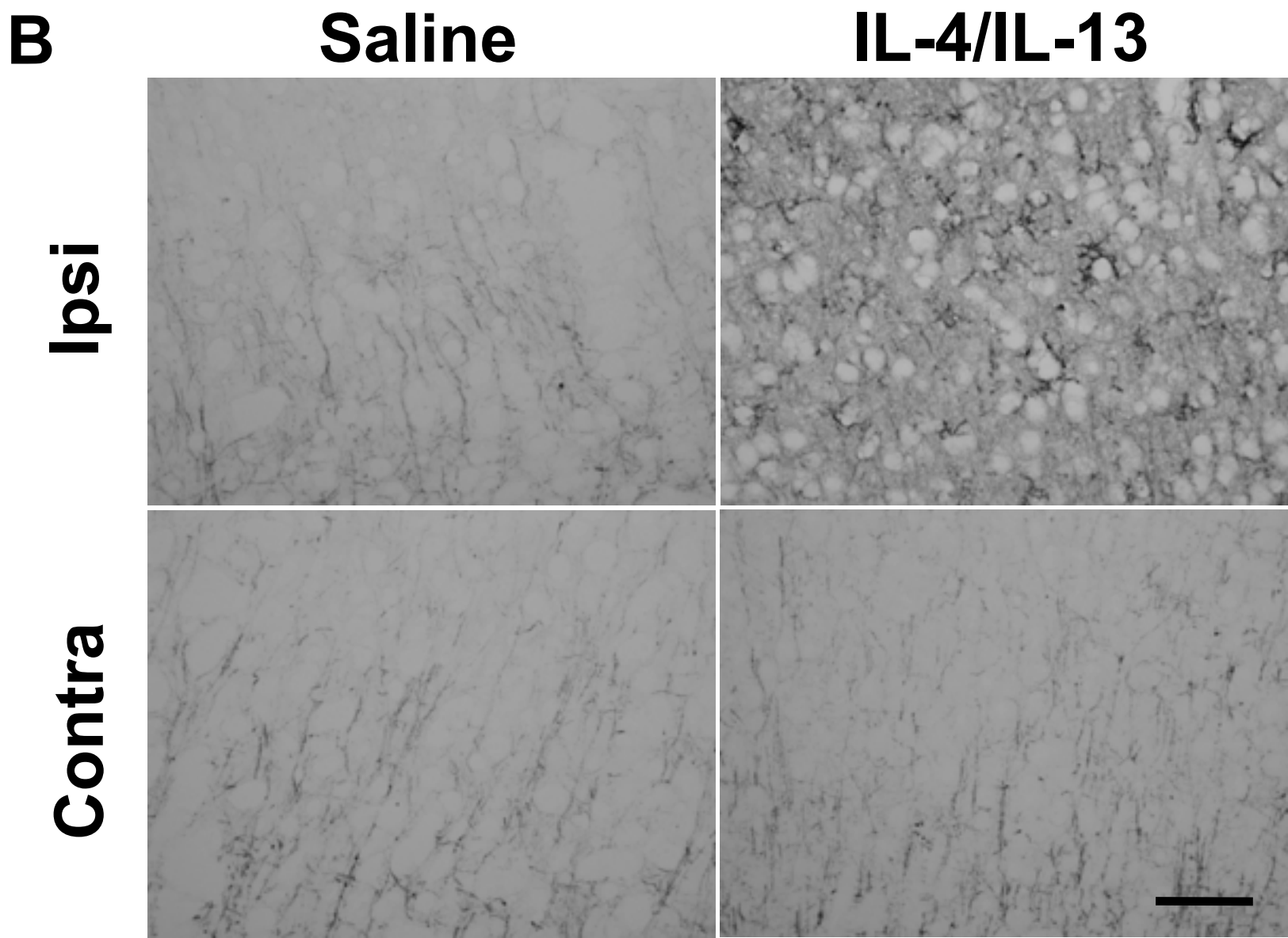
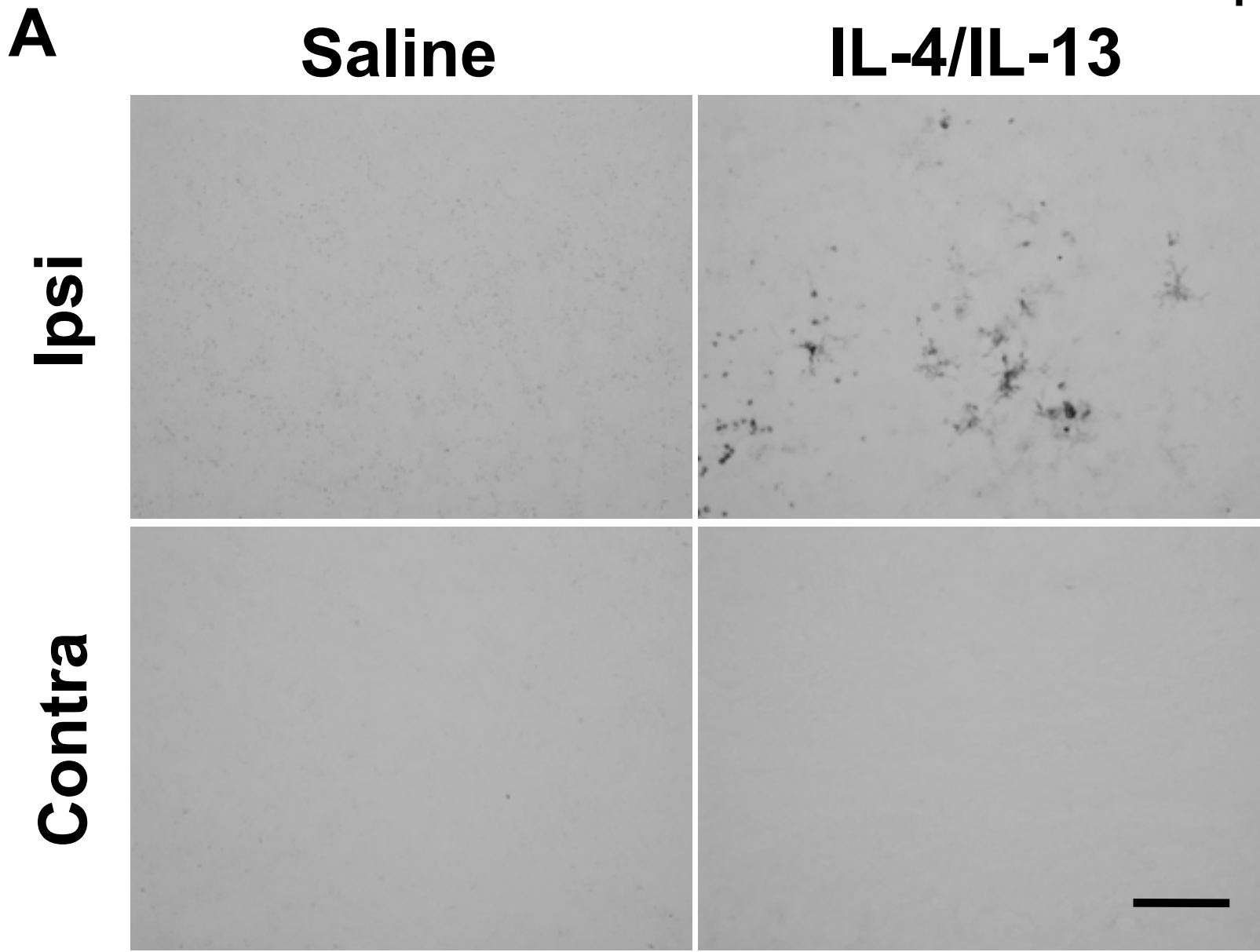


Fig. 7



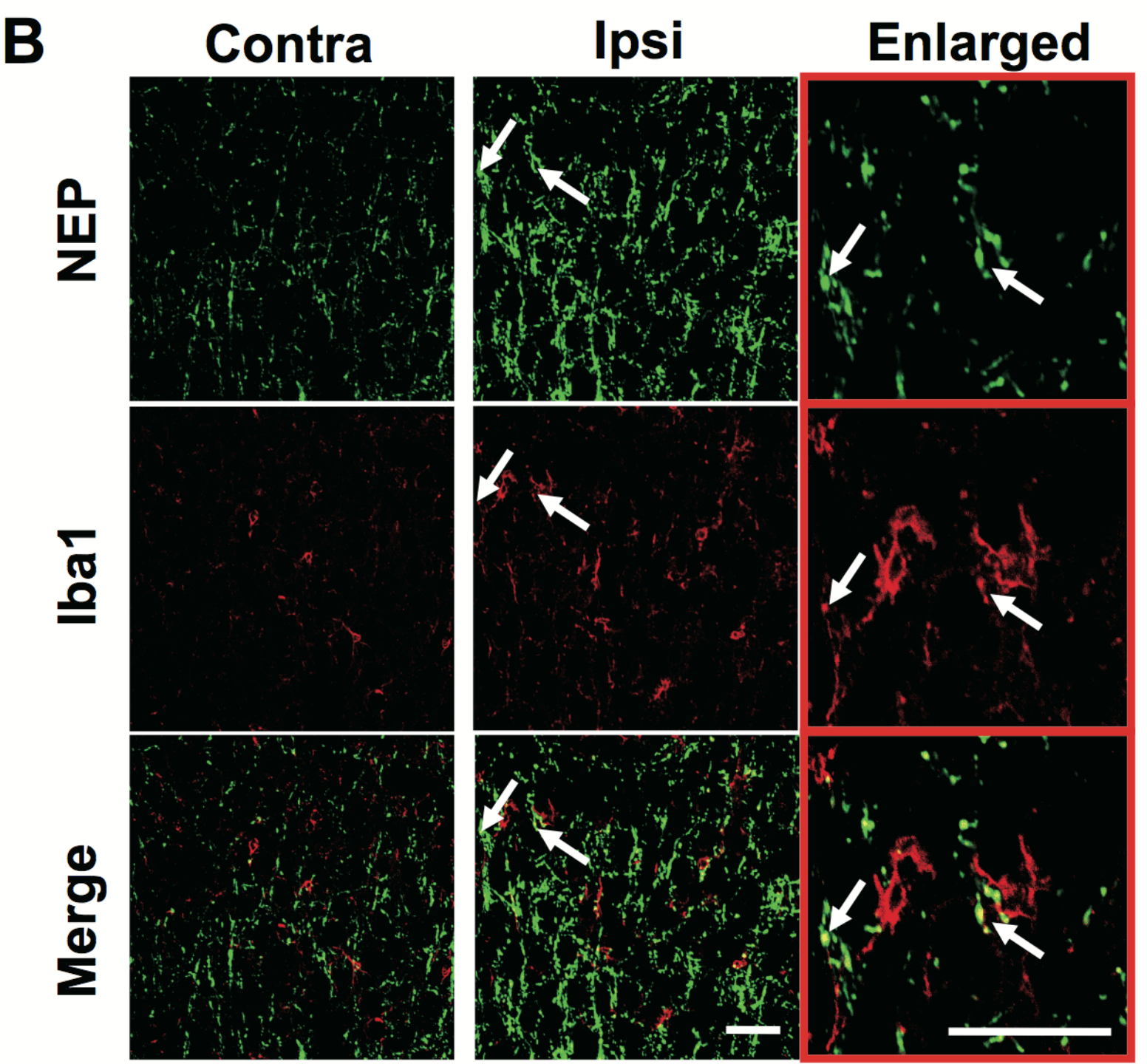
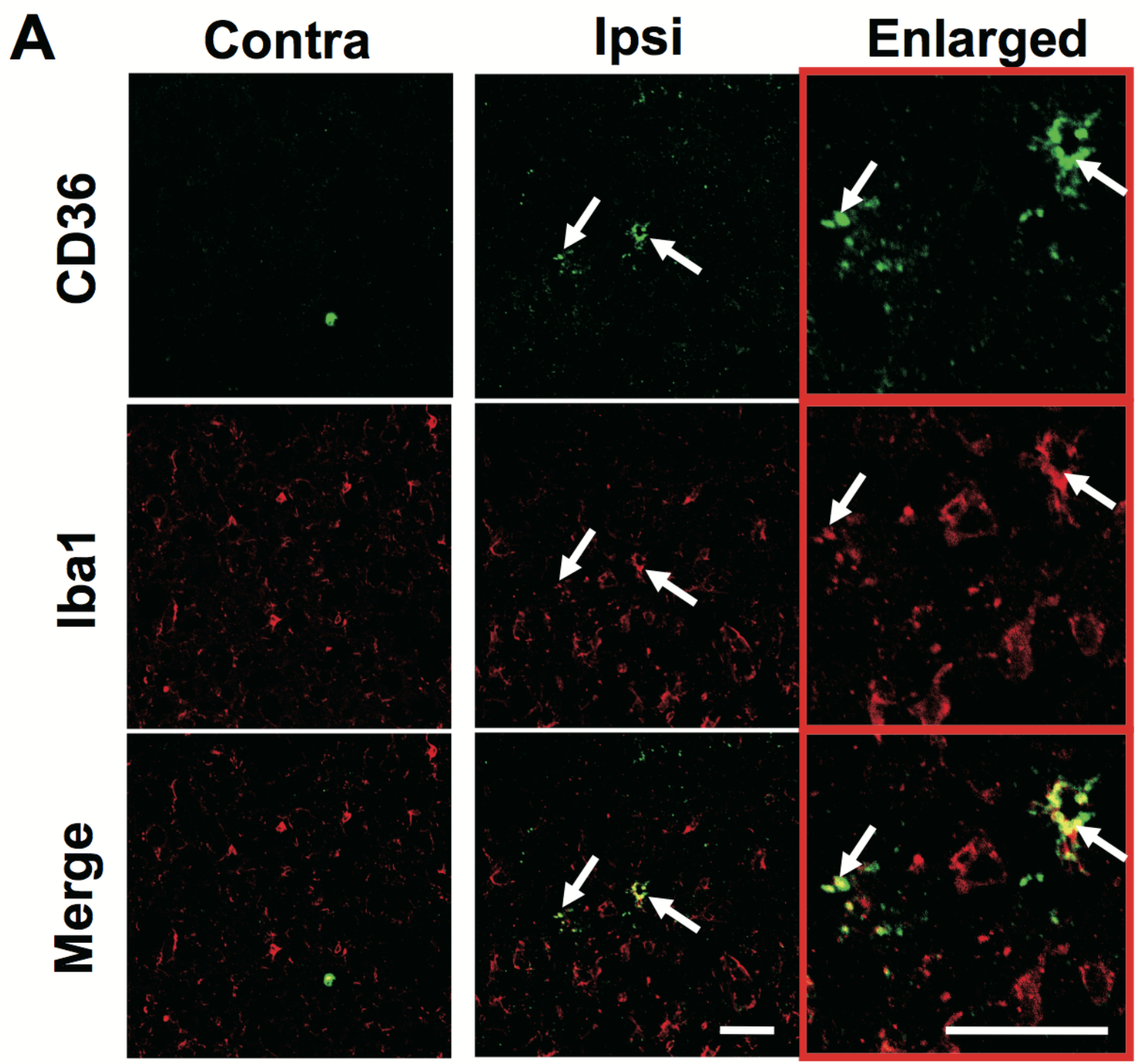


Fig. 9

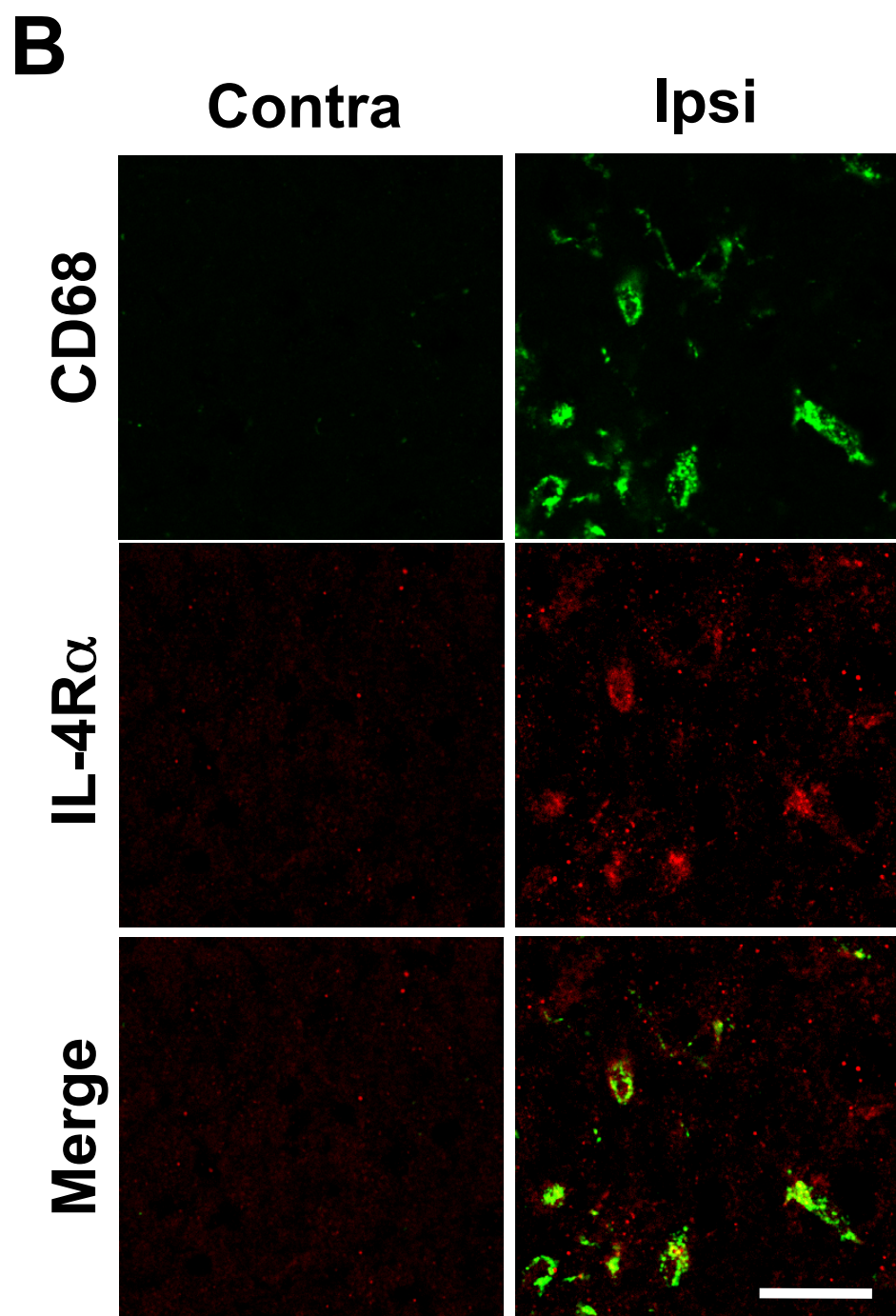
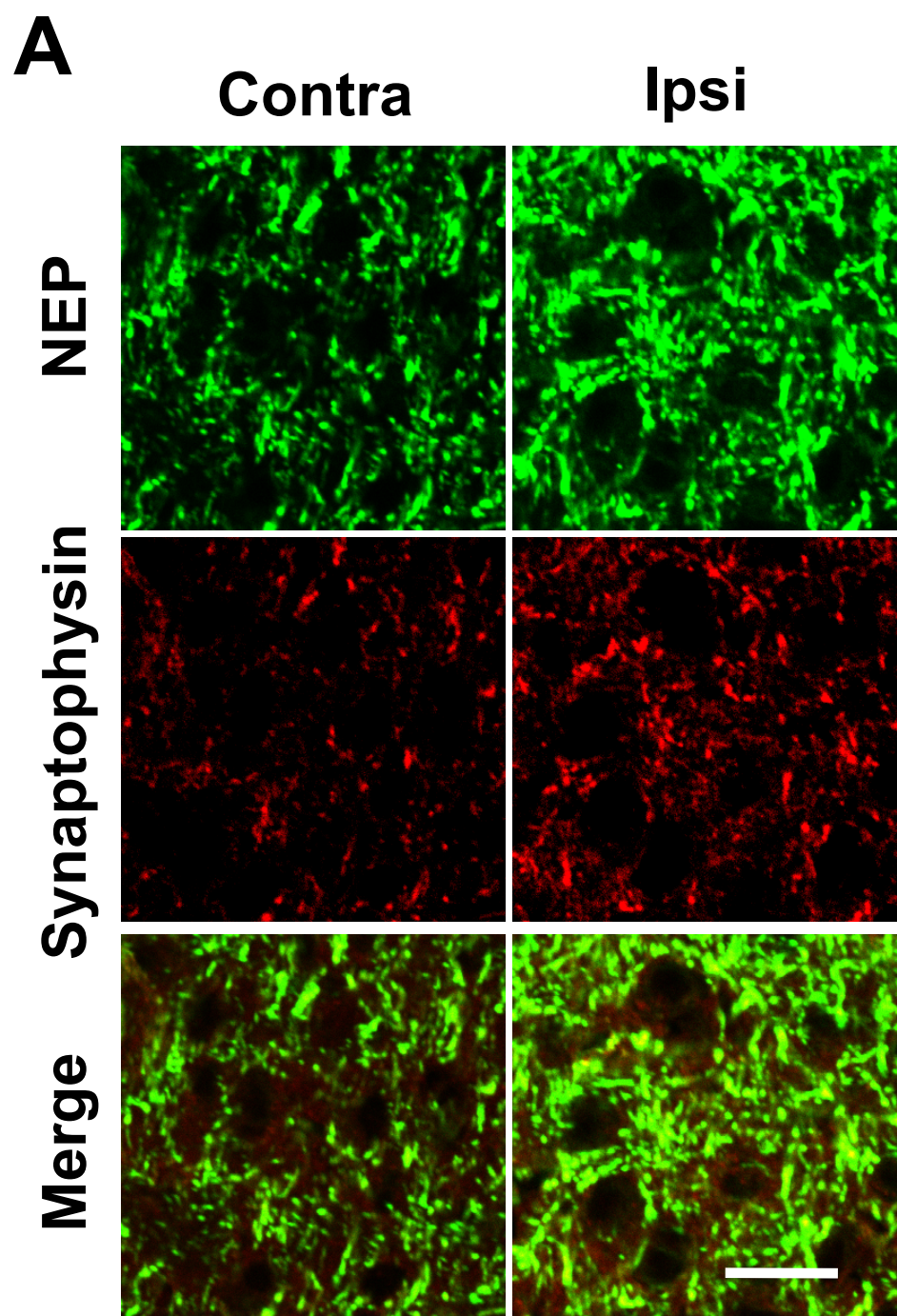


Fig. 10

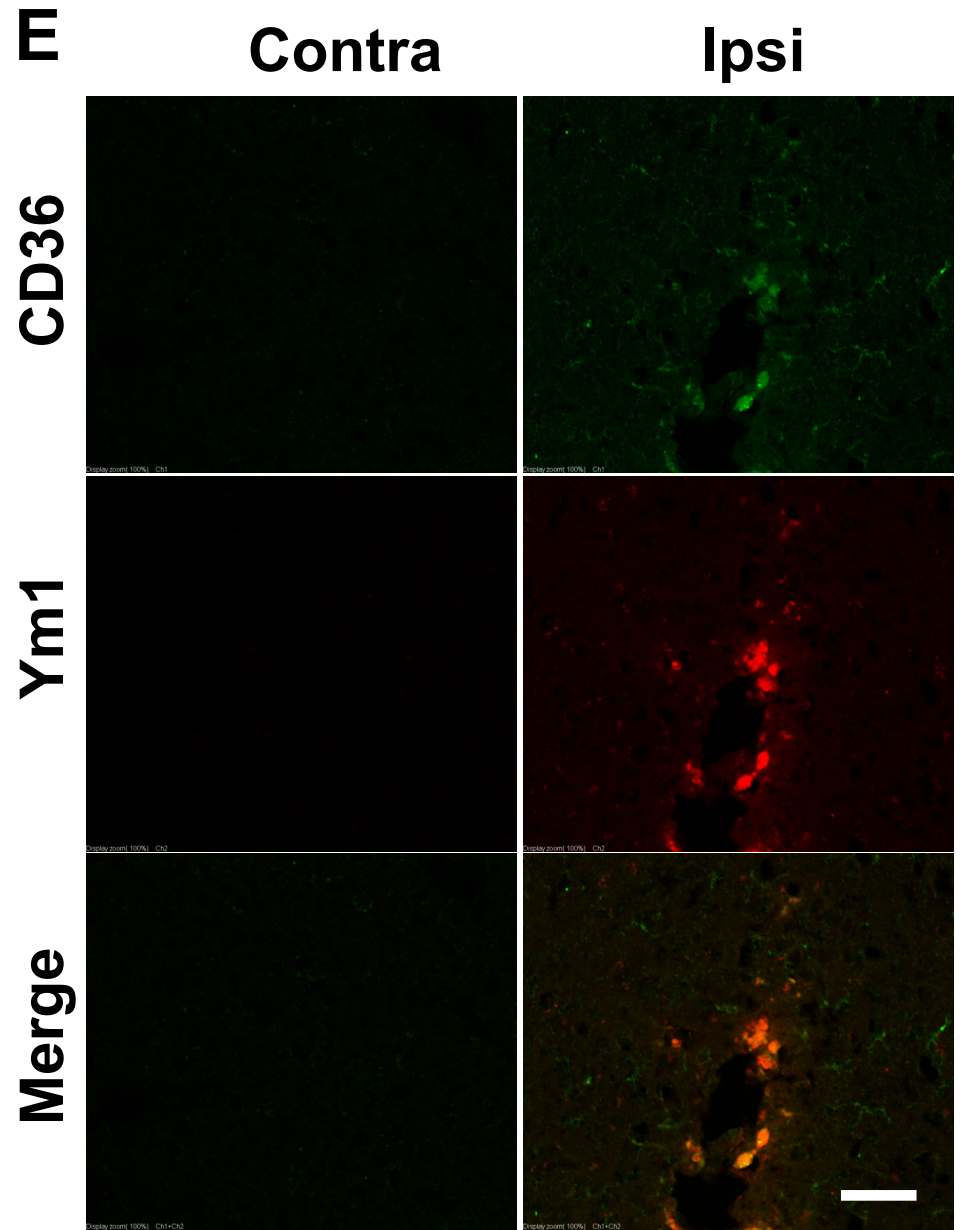
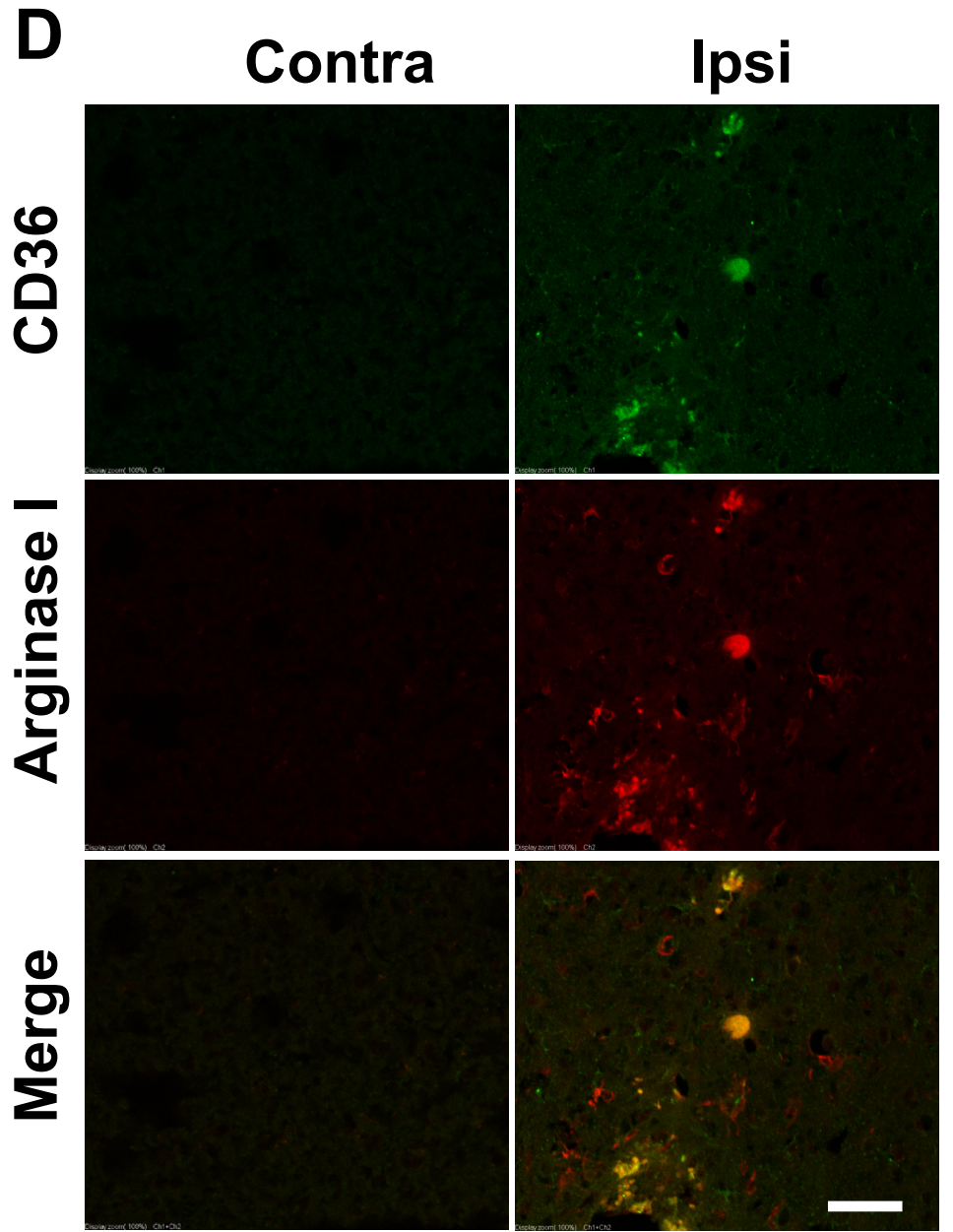
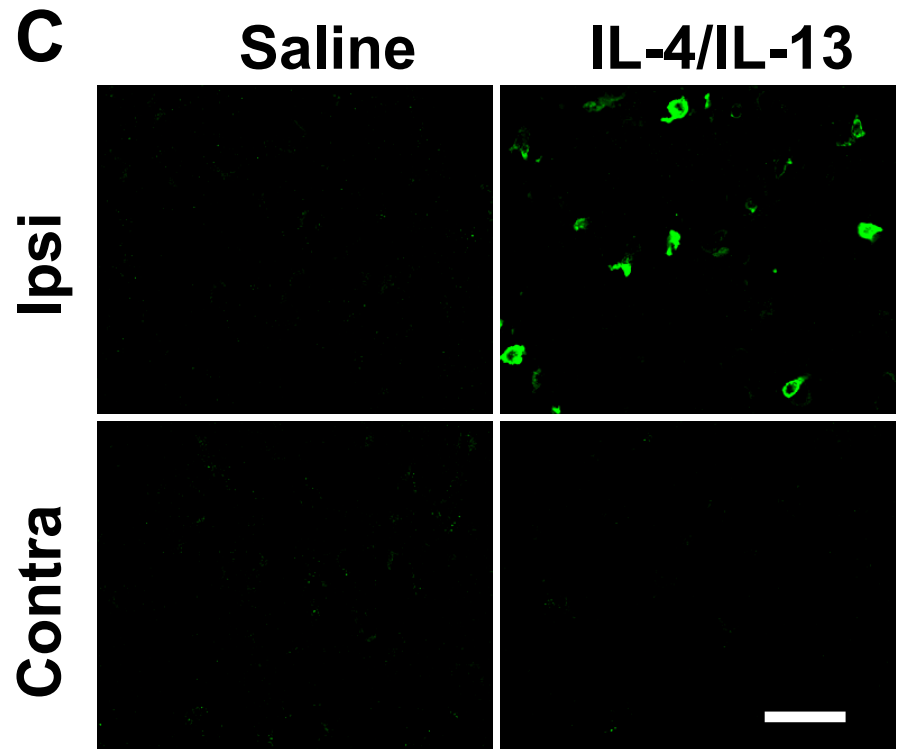
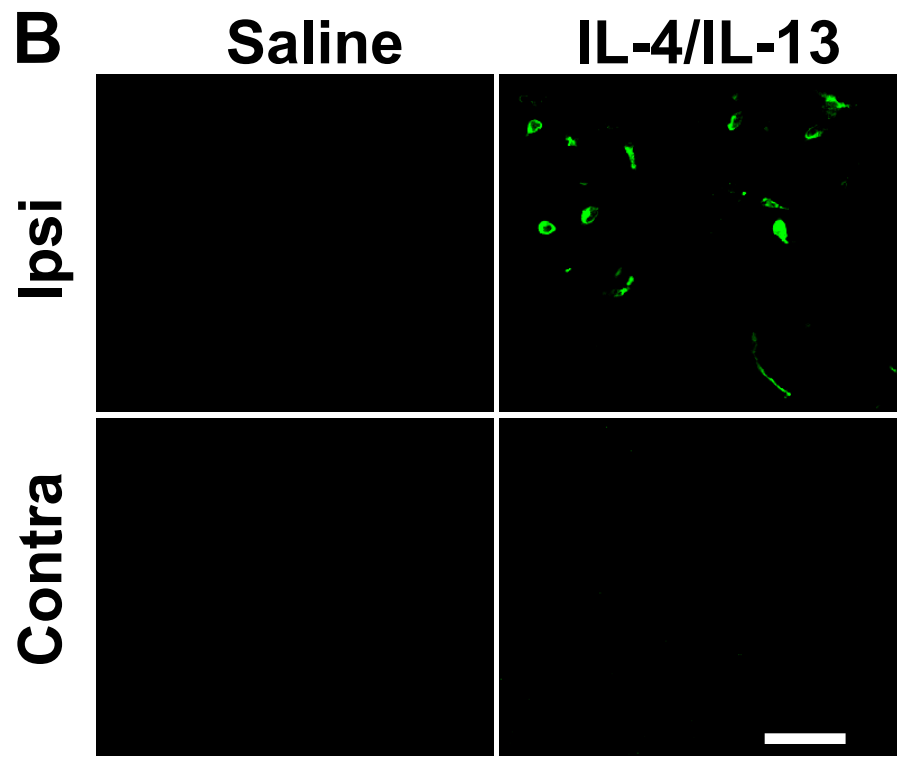
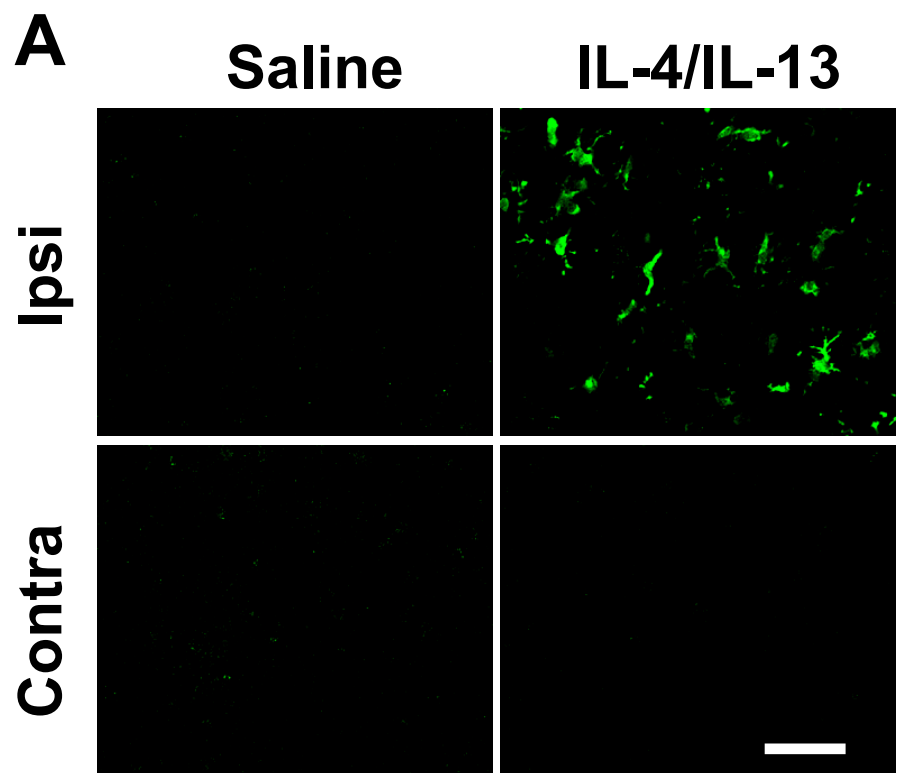


Fig. 11

